

# Bayesian ICA with super-Gaussian Source Priors

**Jyotishka Datta**

*Department of Statistics, Virginia Tech*

JYOTISHKA@VT.EDU

**Soham Ghosh**

*Department of Statistics, University of Wisconsin–Madison*

SGHOSH39@WISC.EDU

**Nicholas G. Polson**

*Booth School of Business, University of Chicago*

NGP@CHICAGOBOOTH.EDU

**Editor:** TBD

## Abstract

Independent Component Analysis (ICA) plays a central role in modern machine learning as a flexible framework for feature extraction. We introduce a horseshoe-type prior with a latent Pólya-Gamma scale-mixture representation, yielding scalable algorithms for both point estimation via expectation–maximization (EM) and full posterior inference via Markov chain Monte Carlo (MCMC). This hierarchical formulation unifies several previously disparate estimation strategies within a single Bayesian framework. We also establish the first theoretical guarantees for hierarchical Bayesian ICA, including posterior contraction and local asymptotic normality results for the unmixing matrix. Comprehensive simulation studies demonstrate that our methods perform competitively with widely used ICA tools. We further discuss implementation of conditional posteriors, envelope-based optimization, and possible extensions to flow-based architectures for nonlinear feature extraction and deep learning. Finally, we outline several promising directions for future work.

**Keywords:** Bayesian ICA, blind source separation, super-Gaussian priors, heavy-tailed shrinkage, Pólya–Gamma mixtures.

## 1 Introduction

Linear independent component analysis (ICA)<sup>1</sup> is central to blind source separation and has many fields of application, e.g., signal processing, medical imaging, machine learning and many others. ICA can be viewed as a feature extraction problem where a random vector  $\mathbf{x}$  with coordinates that admit a representation as linear combination of independent latent variables  $\mathbf{s}$  with an unknown mixing matrix  $\mathbf{A}$ , namely  $\mathbf{x} = \mathbf{As}$ . One needs to estimate  $\mathbf{A}$  or the unmixing matrix  $\mathbf{W} = \mathbf{A}^{-1}$  (Comon et al., 1991; Comon, 1994; Bell and Sejnowski, 1995; Hyvärinen and Pajunen, 1999). ICA can be viewed of as a refinement or an extension of principle component analysis (PCA) or factor analysis, in that the PCA only requires uncorrelated components, not independent.

Feature engineering (a.k.a. nonlinear factor analysis) is a fundamental problem in many modern day machine learning applications ranging from medical imaging to signal processing. A key aspect of feature engineering is decomposing high-dimensional data into independent latent factors. Bhadra et al. (2024) presents a statistical view of high-dimensional deep learning. In this formulation, the output  $\mathbf{Y}$  and input  $\mathbf{X}$  connected via a statistical model:

$$P(\mathbf{Y} \mid \mathbf{W}, \mathbf{X}) = P(\mathbf{Y} \mid \mathbf{a}), \quad \mathbf{a} = \mathbf{WX},$$

where,  $\mathbf{a}$  are linear factors to be extracted, connected via a hierarchical model with no error in the second stage of hierarchy. Linear ICA can be useful here as it separates the observed data into a lower-dimensional array of independent sources (a.k.a. features) to offer a high-dimensional probabilistic structure. Thus, ICA falls into the class of high-dimensional data reduction methods and help one identify pivotal data features as well as yield optimal predictive outcomes. A key feature of popular statistical or machine learning models is that they necessitate an approach that concurrently discerns both the foundational independent features and their associated mixing weights, colloquially termed as nonlinear mixing maps.

Our primary objective is to unify an array of algorithmic approaches to allow for both MAP optimization and fully Bayesian estimation for ICA. Method of moments estimators are commonplace in this literature and have lead to tensor methods. Our work builds on the seminal work of (MacKay, 1992a, 1996) who showed that the (Bell and Sejnowski, 1995) algorithm for signal processing for a non-linear feedforward network can be viewed as a maximum likelihood algorithm for the optimization of a linear generative model.

Our main contributions are: 1. Developing a fully Bayesian ICA framework with horseshoe-type priors, using a Pólya-Gamma-augmented Gaussian scale mixture hierarchy that leads to a simple Gibbs sampler (**Gibbs-ICE**) for posterior inference on the sources and the unmixing matrix. 2. Unifying existing models using Gaussian scale mixture representation. 3. Providing, to our knowledge, the first posterior contraction and Bernstein–von Mises results for hierarchical Bayesian ICA: under known source densities and mild regularity conditions, we establish a uniform LAN expansion for the ICA likelihood and show that the posterior for the unmixing matrix  $\mathbf{W}$  contracts at the parametric rate  $N^{-1/2}$  up to signed permutations, and is asymptotically normal (Section 4). 4. Carrying out an extensive simulation study, including controlled experiments under our generative hierarchy and large-scale benchmarks against contemporary ICA methods. Using a Gibbs sampler (**Gibbs-ICE**) built from our hierarchy, we find that the proposed Bayesian procedures are

---

1. Some authors e.g., Dinh et al. (2014) use the acronym ICE, for Independent Component Estimation.

competitive in terms of Amari distance, source recovery correlation, and reconstruction error across a range of super-Gaussian source families (Sections 5–5.2).

The hallmark of ICA methods is the use of a super-Gaussian distribution over hidden states. Surprisingly, this leads to identification where traditional Gaussian modeling assumptions do not. A linear mixing of Gaussian distribution is itself Gaussian, so de-mixing is impossible. Hence the source distribution must have heavy tails (a.k.a. super-Gaussian). We show that the easiest way to achieve this is via ‘Horseshoe-type’ priors which are heavy-tailed by construction. Horseshoe priors have been a default class of priors for many problems, especially shrinkage estimation in high-dimensional inference, where the marginal density possesses both a spike at zero and regularly varying tails, see [Carvalho et al. \(2010\)](#); [Bhadra et al. \(2016b, 2017\)](#).

Generative models have achieved many successful applications ranging from machine learning to image processing. They can be applied in the context of ICA. To fix notation let the data generating model be constructed as follows: data  $\mathbf{y}$  is generated from a baseline source distribution,  $\mathbf{s} \sim p(\mathbf{s})$  via a latent state  $\mathbf{x}$  which is a ridge function of  $\mathbf{s}$ , namely  $g(\mathbf{As} + \mathbf{b})$  for an activation function  $g(\cdot)$  and then,

$$\mathbf{x} = g(\mathbf{As} + \mathbf{b}), \text{ where } \mathbf{s} \sim p(\mathbf{s}).$$

The mixing matrix  $\mathbf{A}$  provides ‘feature extraction’ – a central problem in machine learning. We consider below the special case  $g = \mathbb{1}(\cdot)$ , the identity map, but  $g$  could be a deep learner with many layers. Training high-dimensional generative models such as LLMs (large language models) is extremely costly and novel scalable algorithms to help in this task are an active area of interest. We refer the readers to [Polson and Sokolov \(2020\)](#); [Tran et al. \(2020\)](#) for a comprehensive review of the computational aspects of deep learning.

Our approach is inspired by the seminal insight of [MacKay \(1992a, 1996\)](#) that ICA can be viewed as a latent variable modeling problem. [MacKay \(1996\)](#) provides instances of many statistical models (e.g., mixture models, hidden Markov models, factor analysis or Helmholtz machines) that are generative models with a layer of latent variables that are usually modeled with simple, separable distributions. Across each of these modeling frameworks, learning the latent variables is tantamount to describing the observables in terms of independent components, and hence, it is natural to expect that ICA should also admit a generative latent variable representation. With this interpretation, [MacKay \(1992a\)](#) shows that the original blind separation algorithm of [Bell and Sejnowski \(1995\)](#) can be viewed as a maximum a posteriori (MAP) estimator from the marginalized likelihood, where the trick is to write the ICA as a latent variable model with a separable distribution on the hidden states. In this representation, the latent variables are assumed to be mutually independent and non-Gaussian, and are called independent components. The key insight then that underlies our unifying approach is that the components of the source distribution can be modeled with scale mixtures of normals ([West, 1987](#); [Barndorff-Nielsen et al., 1982](#)). We show that MacKay’s original model and its extensions are simply scale mixtures with Pólya-Gamma mixing ([Polson et al., 2013](#)) and are thus horseshoe-type priors ([Polson and Scott, 2012a, 2013](#)).

On the algorithmic side, we show that a number of hitherto disjoint algorithms can be unified as envelope optimization methods (see [Geman and Yang, 1995](#); [Polson and Scott, 2016](#)). For example, the ICA updating scheme due to [Bell and Sejnowski \(1995\)](#) is equivalent

to a maximum likelihood approach, see (MacKay, 1992a, 1996). Auxiliary variable methods allow for both EM and MCMC algorithms to be developed across a wide spectrum of source distributions. Such methods can lead to faster convergence (Ono and Miyabe, 2010) and can incorporate methods for fast convergence such as Nesterov acceleration and block-coordinate descent, thus providing an alternative to traditional stochastic gradient descent methods.

From a historical perspective, Independent Component Analysis arises as a possible solution to the ‘Blind source separation’ problem, a classical problem in signal processing. In the formulation by (Herault and Jutten, 1986; Bell and Sejnowski, 1995), algorithms for blind source separation attempt to recover source signals  $\mathbf{s}$  from observations  $\mathbf{x}$ , where  $\mathbf{x} = \mathbf{Vs}$ , are linear mixtures with unknown weights  $\mathbf{V}$ . This is done by finding a square matrix  $\mathbf{W}$  which is the inverse of the mixing matrix  $\mathbf{V}$ , up to permutation and change of scale. For example, (Bell and Sejnowski, 1994, 1995) take an algorithmic approach summarized as a linear mapping  $\mathbf{a} = \mathbf{Wx}$  where  $\mathbf{a}$  is an estimate of the source signals. This is done by adjusting the unmixing matrix  $\mathbf{W}$  to maximize the entropy of the outputs.

The algorithm proceeds iteratively using a gradient ascent method on the log-likelihood of the estimated sources, where the update rule for  $\mathbf{W}$  is:

$$\nabla \mathbf{W} \propto (I - 2\phi(\mathbf{a})\mathbf{a}^T) \mathbf{W}$$

where,  $I$  is the identity matrix, and  $\phi(\mathbf{a})$  is a non-linear function applied component-wise to  $\mathbf{a}$ . Common choices for  $f$  are the logistic sigmoid function or the hyperbolic tangent (i.e., a nonlinear map  $\mathbf{z}_i = \phi_i(\mathbf{a}_i)$  where  $\phi(\cdot) = -\tanh(\cdot)$ ).

A Bayesian approach (Févotte et al., 2004; Févotte and Godsill, 2006; Donnat et al., 2019; MacKay, 1992a) has a two-fold advantage. First, rather than casting problem as a method of moments approach (kurtosis), a Bayesian approach finds the solution by a suitable regularization with a heavy-tailed prior (thus imposing constraint on higher order moments). A particular suitable class is super-Gaussian priors (Palmer et al., 2006) via scale mixtures of normals (West, 1987). MacKay (1992a) uses a heavy-tailed source distribution towards this. The advantage is that mixture and envelope methods can be used to extract features/factors and provide fast scalable algorithms for ICA. In this paper, we unify the existing Bayesian algorithms and provide new ones.

Assuming a source distribution,  $\mathbf{s} \sim p(\mathbf{s})$  acts as a regularization penalty and allows us to unify existing procedures as MAP estimators. For example, MacKay (1996) shows that if  $\phi_i(a_i) = -\tanh(a_i)$  then this is equivalent to a source distribution of the form  $p_i(s_i) \propto 1/\cosh(s_i) = 1/(e^{s_i} + e^{-s_i})$ . We argue in section 2 that this can be written as a Gaussian scale mixture using a Pólya-Gamma mixing density. Moreover, (MacKay, 1992b) suggests adding a gain  $\beta$  and considering a heavy-tailed source distribution of the form  $p_i(s_i) \propto 1/\cosh^{1/\beta}(\beta s_i)$ . Again we show that this can be represented as a Normal scale mixture thus leading to classes of auxiliary variable methods for inference and optimisation. In the limit as  $\beta \rightarrow \infty$  this becomes  $p_i(s_i) \propto \exp(-|s_i|)$  the double exponential (a.k.a. Lasso) prior, and as  $\beta \rightarrow 0$ ,  $p_i(s_i)$  would converge to a zero-mean Gaussian with variance  $1/\beta$ .

A related goal is to bring together the modeling of source distributions under the encompassing paradigm of Gaussian scale mixtures (Andrews and Mallows, 1974; West, 1987; Carlin and Polson, 1991). This latent variable or parameter expansion approach offers fast, scalable algorithms akin to the auxiliary variable methods proposed by (Ono and Miyabe, 2010). Furthermore, it obviates dependence on approximative techniques like variational

Bayes (VB). Our methodology bears significance for deep Bayesian models wherein latent variable distributions are forged as superpositions of nonlinear mappings, akin to deep learning constructs (Polson and Sokolov, 2017; Polson and Rovcková, 2018).

On the theoretical side, Section 4 makes this link precise by formulating the ICA likelihood as a finite-dimensional parametric model indexed by the unmixing matrix and proving a uniform LAN expansion around the true  $W_0$ . This leads to  $\sqrt{N}$ -rate posterior contraction in a signed-permutation invariant metric  $d_{\pm}$  and a Bernstein–von Mises theorem for  $\text{vec}(W)$ , thus providing a matrix-level asymptotic normality result for ICA in a hierarchical Bayesian framework. On the empirical side, Section 5 and Section 5.2 show that our Pólya-Gamma-augmented Gibbs sampler gives practically competitive performance relative to established ICA algorithms across a range of super-Gaussian source distributions and noise levels.

The rest of our paper is outlined as follows. The next subsection describes connections with previous work. Section 2 provides a discussion of deep Bayesian generative models. Section 3 provides a unifying framework for super-Gaussian source distributions. Section 4 develops our posterior contraction and Bernstein–von Mises results for the unmixing matrix. Section 5–5.2 illustrate our methodology through numerical experiments and extensive comparisons with contemporary ICA methods. Finally, Section 6 concludes with directions for future research.

## 1.1 Connections with Previous Work

As Auddy and Yuan (2023) point out, the mixing matrix  $\mathbf{A}$  can be identified up to permutation and scaling under the assumption of at most one Gaussian component in  $\mathbf{S}$  due to a theorem by Comon (1994). The review paper Auddy et al. (2024) demonstrates that this can also be connected with the Kruskal identifiability theorem (Kruskal, 1977) that shows a remarkable difference between matrix and tensors: while a matrix of rank  $\rho$  can be decomposed in many ways as a sum of  $\rho$  rank-one matrices, but higher-order tensors typically admit unique decomposition into rank-one tensors. In the context of PCA versus ICA, Auddy et al. (2024) observe that the the principal components are singular vectors of covariance matrix, while the independent components are ‘singular vector’s of fourth order cumulant tensors, and hence, PCA can not reconstruct independent random variables with mean zero, unit variance but non-zero excess kurtosis, but ICA can. There have been many approaches for solving the ICA problem including but not limited to (MacKay, 1992a; Comon, 1994; Bell and Sejnowski, 1995; MacKay, 1996; Deco and Obradovic, 1996; Hyvärinen and Pajunen, 1999; Hastie and Tibshirani, 2002b; Ono and Miyabe, 2010; Samworth and Yuan, 2012; Auddy and Yuan, 2023) as well as hierarchical Bayesian approaches such as MacKay (1992a); Févotte et al. (2004); Févotte and Godsill (2006); Karklin and Lewicki (2005); Asaba et al. (2018). We refer the readers to Hyvärinen et al. (2001); Nordhausen and Oja (2018) for comprehensive reviews.

Samworth and Yuan (2012) proposes a nonparametric maximum likelihood approach for estimating the unmixing weights and the marginal distributions by projecting the empirical distributions on the space of log-concave univariate distributions. They also address the question of identifiability of the unmixing matrices, first studied by Comon (1994), and in their formulation identifiability up to scaling and permutation is guaranteed by requiring that not more than one of the univariate log-concave projections is Gaussian. This is

also connected to Kruskal's identifiability conditions (Kruskal, 1977) for a tensor product  $T = \sum_{r=1}^R A \otimes B \otimes C$ , in terms of the Kruskal ranks of the individual matrices:  $\kappa_A + \kappa_B + \kappa_C \geq 2R + 2$ . Bhaskara et al. (2014) provide a robust version of the identifiability theorem for approximate recovery and point uses in several latent variable models. We refer the readers to the comprehensive review by Audy et al. (2024) on tensor methods for high-dimensional data analysis.

Camuto et al. (2021) combine a linearly independent component analysis (ICA) with nonlinear bisective feature maps (from flow-based methods). For non-square ICA, they can assume the number of sources is less than the data dimensionality – thus achieving better unsupervised latent factor discovering than other ICA flow-based methods. Dinh et al. (2014) discuss nonlinear independent component estimation (NICE), deep generative models with nonlinear invertible neural networks, building on the work of Deco and Obradovic (1996), Obradovic and Deco (1998), Comon et al. (1991) and Pearlmuter and Parra (1996) and Malthouse (1998). Recent work includes Bayesian ICA models of (Donnat et al., 2019). Other related approaches include auto-encoder and sparsity models.

Nonlinear ICA models have been proposed by Hyvärinen and Pajunen (1999), although identification can be challenging. Khemakhem et al. (2020) provides recent identification results, providing mild conditions under which the joint distribution encompassing both observed and latent variables within Variational Autoencoders (VAEs) are identifiable and estimable, thus establishing a connection between VAEs and nonlinear Independent Component Analysis (ICA). The source  $\mathbf{S}$  is a feature vector that needs to be learned, see, for example, Olshausen and Field (1996, 1997) for sparse coding of natural images, where an image is modeled as a natural superposition using an over-complete basis set where the amplitudes are given sparsity-inducing prior distributions. This is based on the intuition of Barlow's principle of redundancy reduction (Barlow, 1989, 2001).

Other popular approaches for dimension reduction include Sliced Inverse Regression (Li, 1991) that finds a low-dimensional projection of the data that captures the most relevant information for explaining the variation in the data, specifically designed for non-linear relationships in the data. Unlike traditional linear dimensionality reduction methods like Principal Component Analysis (PCA). Lopes et al. (2012) introduces a sequential online strategy for efficient posterior simulation. Finally, as noted by Brillinger (2012) and Naik and Tsai (2000), the mixing matrix can be consistently estimated through PLS, regardless of the activation function's nonlinearity, albeit with a proportionality constant. While the assumption by Brillinger (2012) of Gaussian input  $\mathbf{X}$  is necessary for applying Stein's lemma, we note that this outcome extends to scale-mixtures of Gaussians.

## 2 Hierarchical Independent Components Analysis

### 2.1 The generative model and the likelihood function

We begin with linear independent component models. The goal of ICA is to attempt to recover source signals  $\mathbf{S}$  from observations  $\mathbf{X}$  which are linear mixtures (with unknown coefficients  $\mathbf{A}$ ) of the source signals, i.e.  $\mathbf{X} = \mathbf{AS}$ , where  $\mathbf{W} = \mathbf{A}^{-1}$ . This can be interpreted as a Bayesian hierarchical model with a degenerate first stage. We follow MacKay (1996)'s formulation here. We observe data as  $N$  observations  $\mathbf{x}^{(n)}$ ,  $1 \leq n \leq N$ , which are linear mixtures of sources  $\mathbf{s}^{(n)}$ . Let  $\mathbf{s}^{(n)} \in \mathbb{R}^d$ ,  $1 \leq n \leq N$ , denote the set of sources, that are

independently distributed with marginal density  $p_i(s_i^{(n)})$ , so that

$$\mathbf{x}^{(n)} = \mathbf{A}\mathbf{s}^{(n)} \quad \text{with} \quad p(\mathbf{s}^{(n)}) = \prod_{i=1}^d p_i(s_i^{(n)}),$$

where  $\mathbf{A}$  is the mixing matrix. We wish to estimate  $\mathbf{W} = \mathbf{A}^{-1}$ . As stated before, the sources  $\mathbf{s}^{(n)}$  have an independent components distribution and can be viewed as latent variables. The joint probability of the observed and the hidden latent variables can be written as

$$\begin{aligned} p(\{\mathbf{x}^{(n)}\}_{n=1}^N, \{\mathbf{s}^{(n)}\}_{n=1}^N \mid \mathbf{A}) &= \prod_{n=1}^N p(\mathbf{x}^{(n)} \mid \mathbf{s}^{(n)}, \mathbf{A}) p(\mathbf{s}^{(n)}) \\ &= \prod_{n=1}^N \left\{ \prod_{i=1}^d \delta\left(x_i^{(n)} - \sum_{j=1}^d A_{ij} s_j^{(n)}\right) \right\} \prod_{j=1}^d p_j(s_j^{(n)}), \end{aligned} \quad (1)$$

where  $\delta(\cdot)$  denotes the Dirac delta function. [MacKay \(1996\)](#) points out that it is straightforward to replace  $\delta(x_j^{(n)} - \sum_i A_{ji} s_i^{(n)})$  with a probability distribution over  $x_j^{(n)}$  with mean  $\sum_i A_{ji} s_i^{(n)}$ , but we need to assume  $\mathbf{x}$  is generated without noise to obtain the [Bell and Sejnowski \(1995\)](#) algorithm exactly.

To access a wider range of probability densities, we can introduce auxiliary variables  $\lambda$  such that

$$p(\mathbf{s}^{(n)}) = \int p(\mathbf{s}^{(n)} \mid \lambda) p(\lambda) d\lambda.$$

Gaussian scale mixtures ([West, 1987](#); [Bhadra et al., 2016a](#)) encompass a wide range of commonly used prior distributions in Bayesian literature, and are also a source of constructing newer priors for handling data with sparsity or other structures. In fact, it is easy to see that the existing prior distributions for Bayesian ICA, viz. Student's  $t$  ([Févotte et al., 2004](#)), Jeffreys' prior  $p(s_i) \propto 1/|s_i|$  ([Févotte and Godsill, 2006](#)), or Laplace ([Asaba et al., 2018](#)), are all Gaussian scale mixtures. We will argue later in the section that one can recover [MacKay \(1992a\)](#)'s hyperbolic secant distribution as a Gaussian scale mixture, too. This has many theoretical and practical advantages. For example, in designing computational algorithms, we can develop EM and MCMC algorithms using the joint posterior  $p(\mathbf{s}^{(1:N)}, \lambda \mid \mathbf{x}^{(1:N)})$ . We also know a great deal about the behavior of Gaussian scale mixtures due to the works of [Barndorff-Nielsen et al. \(1982\)](#) and others.

To obtain the maximum likelihood estimator under the noiseless model, we first observe that the likelihood can be obtained as a product of the following factors from (1), for  $n = 1, \dots, N$ :

$$p(\mathbf{x}^{(n)} \mid \mathbf{A}) = \int p(\mathbf{x}^{(n)} \mid \mathbf{A}, \mathbf{s}^{(n)}) p(\mathbf{s}^{(n)}) d\mathbf{s}^{(n)} = \int \left\{ \prod_{i=1}^d \delta\left(x_i^{(n)} - \sum_{j=1}^d A_{ij} s_j^{(n)}\right) \right\} \prod_{i=1}^d p_i(s_i^{(n)}) d\mathbf{s}^{(n)}.$$

We use the summation convention like [MacKay \(1996\)](#), i.e.,  $A_{ij} s_j^{(n)} \equiv \sum_{j=1}^d A_{ij} s_j^{(n)}$ . Now, using the elementary fact that

$$\int \delta(\mathbf{x} - \mathbf{A}\mathbf{s}) f(\mathbf{s}) d\mathbf{s} = |\mathbf{A}|^{-1} f(\mathbf{W}\mathbf{x}), \quad \mathbf{W} = \mathbf{A}^{-1},$$

we obtain the likelihood (and log-likelihood) for a single term:

$$p(\mathbf{x}^{(n)} | \mathbf{A}) = \frac{1}{|\mathbf{A}|} \prod_{i=1}^d p_i((\mathbf{A}^{-1} \mathbf{x}^{(n)})_i) = \prod_{i=1}^d p_i(W_{ij} x_j^{(n)}) |\mathbf{W}|,$$

$$\Rightarrow \log p(\mathbf{x}^{(n)} | \mathbf{A}) = \log |\mathbf{W}| + \sum_{i=1}^d \log p_i(W_{ij} x_j^{(n)}) \doteq \log |\mathbf{W}| + \sum_{i=1}^d \log p_i(a_i), \text{ where } a_i \equiv W_{ij} x_j^{(n)}.$$

We can then optimize the log-likelihood using any gradient or envelope method. The terms  $\phi_i(a_i) = d \log p_i(a_i) / da_i$  are key here and indicate the gradient direction for maximum likelihood.

We mention two key points in [MacKay \(1996\)](#), (Section 2.4, points 2 and 3)) here:

1. Employing a tanh nonlinearity of the form  $\phi_i(a_i) = -\tanh(a_i)$  implicitly assumes a probability distribution for latent variables,  $p_i(s_i) \propto 1/\cosh(s_i) \propto 1/(e^{s_i} + e^{-s_i})$ . This distribution exhibits heavier tails compared to the Gaussian distribution, offering a broader range of potential tail behaviors.
2. Alternatively, by incorporating a tanh non-linearity with a gain parameter  $\beta$ , denoted as  $\phi_i(a_i) = -\tanh(\beta a_i)$ , the associated probabilistic model varies with  $\beta$ . The resulting distribution is expressed as  $p_i(s_i) \propto 1/[\cosh(\beta s_i)]^{1/\beta}$ . As  $\beta$  becomes large, the non-linearity converges to a step function, resulting in a Laplace density  $p_i(s_i) \propto \exp(-|s_i|)$ . Conversely, as  $\beta$  approaches zero,  $p_i(s_i)$  tends towards a Gaussian distribution with a mean of zero and a variance of  $\frac{1}{\beta}$ .

**Remark 1 Time versus Transfer Domain.** *It is worthwhile to note that separation in transfer domain is equivalent to separation in the time domain due to the one-to-one mapping between the models in time and transfer domain. Using the notations in [Févotte and Godsill \(2006\)](#); [Févotte et al. \(2004\)](#), the linear instantaneous model in time domain is given by the following model where observations at time  $t$  are noisy combinations of sources at  $t$ , for signals of length  $N$ :*

$$\mathbf{x}_t = \mathbf{A}\mathbf{s}_t + \boldsymbol{\varepsilon}_t, \quad t = 0, \dots, N-1, \quad (2)$$

where  $\mathbf{x}_t = (x_{1t}, x_{2t}, \dots, x_{dt})^\top$  are the observation vectors,  $\mathbf{s}_t = (s_{1t}, s_{2t}, \dots, s_{dt})^\top$  are the sources and  $\boldsymbol{\varepsilon}_t = (\epsilon_{1t}, \epsilon_{2t}, \dots, \epsilon_{dt})^\top$  are the additive noises. The goal is to estimate  $\mathbf{s}_t$  and  $\mathbf{A}$ . We assume that there is a basis  $N \times N$  matrix  $\Phi$  such that sources have a sparse representation on it. The equivalent model in the transfer domain is then

$$\mathbf{x}^{(n)} = \mathbf{A}\mathbf{s}^{(n)} + \boldsymbol{\varepsilon}^{(n)}, \quad n = 0, \dots, N-1, \quad (3)$$

where  $n$  is the coefficient index in the basis decomposition. Separation using (2) and (3) are equivalent since  $\Phi$  is a basis matrix.

## 2.2 Exponential family representation and the posterior

We now show the general derivation for the posterior under the aforementioned hierarchical model for the observables and the latent variables in a noisy linear setting. To reduce

notational clutter, we drop the superscript  $(n)$  and adopt summation convention as needed. Consider

$$\mathbf{x} = \mathbf{A}\mathbf{s} + \boldsymbol{\varepsilon}, \quad \boldsymbol{\varepsilon} \sim \mathcal{N}_d(\mathbf{0}, \sigma^2 \mathbf{I}_d),$$

with prior  $p(\mathbf{s})$  for the sources. The likelihood  $p(\mathbf{x} \mid \mathbf{s})$  derived from this model together with the source distribution  $p(\mathbf{s})$  can be combined to form the posterior of  $\mathbf{s}$  given  $\mathbf{x}$ :

$$\begin{aligned} p(\mathbf{s} \mid \mathbf{x}) &= \frac{1}{(2\pi\sigma^2)^{d/2}} \exp \left\{ -\frac{1}{2\sigma^2} (\mathbf{x} - \mathbf{A}\mathbf{s})^\top (\mathbf{x} - \mathbf{A}\mathbf{s}) \right\} p(\mathbf{s}) \\ &= h(\mathbf{s}) \exp \left\{ \boldsymbol{\eta}^\top \mathbf{s} - \frac{1}{2\sigma^2} \mathbf{x}^\top \mathbf{x} - \log f(\mathbf{x}) \right\} \\ &= h(\mathbf{s}) \exp \left\{ \boldsymbol{\eta}^\top \mathbf{s} - \psi(\boldsymbol{\eta}) \right\}, \end{aligned}$$

where the different components (known functions) are given by

$$\boldsymbol{\eta} = \frac{1}{\sigma^2} \mathbf{A}^\top \mathbf{x} \quad (\text{canonical parameter}),$$

$$\psi(\boldsymbol{\eta}) = \frac{1}{2\sigma^2} \mathbf{x}^\top \mathbf{x} + \log f(\mathbf{x}) = \frac{\sigma^2}{2} \boldsymbol{\eta}^\top \mathbf{W} \mathbf{W}^\top \boldsymbol{\eta} + \log f(\sigma^2 \mathbf{W}^\top \boldsymbol{\eta}) \quad (\text{cumulant function}),$$

$$\text{where } f(\mathbf{x}) = \int h(\mathbf{s}) \exp \left\{ \boldsymbol{\eta}^\top \mathbf{s} - \frac{1}{2\sigma^2} \mathbf{x}^\top \mathbf{x} \right\} d\mathbf{s}, \quad \text{and}$$

$$h(\mathbf{s}) = \frac{1}{(2\pi\sigma^2)^{d/2}} \exp \left\{ -\frac{1}{2\sigma^2} \mathbf{s}^\top \mathbf{A}^\top \mathbf{A}\mathbf{s} \right\} p(\mathbf{s}).$$

Therefore, we can calculate the posterior mean of  $\mathbf{s}$  given  $\mathbf{x}$  as

$$\begin{aligned} \mathbb{E}(\mathbf{s} \mid \mathbf{x}) &= \frac{\partial \psi(\boldsymbol{\eta})}{\partial \boldsymbol{\eta}} = \mathbf{W}\mathbf{x} + \sigma^2 \mathbf{W} \frac{\partial}{\partial \mathbf{x}} \log f(\mathbf{x}) = \frac{\int h(\mathbf{s}) \exp\{\boldsymbol{\eta}^\top \mathbf{s}\} \mathbf{s} d\mathbf{s}}{\int h(\mathbf{s}) \exp\{\boldsymbol{\eta}^\top \mathbf{s}\} d\mathbf{s}}, \\ \frac{\partial}{\partial \mathbf{x}} \log f(\mathbf{x}) &= \frac{1}{\sigma^2} \left( \mathbf{A} \frac{\int h(\mathbf{s}) \exp\{\boldsymbol{\eta}^\top \mathbf{s}\} \mathbf{s} d\mathbf{s}}{\int h(\mathbf{s}) \exp\{\boldsymbol{\eta}^\top \mathbf{s}\} d\mathbf{s}} - \mathbf{x} \right). \end{aligned}$$

We will use this later when deriving a full MCMC algorithm in Appendix B for uncertainty in ICA models.

### 3 Super-Gaussian Source Distributions

As discussed earlier, it is well known that one needs to use a heavy-tailed super-Gaussian distribution as prior for the sources  $\mathbf{s}$  to identify the mixing matrix  $\mathbf{A}$ . In addition, as Févotte et al. (2004) point out, while the over-determined case (number of sensors  $\geq$  number of sources) is relatively easy: there are many efficient approaches, especially within Independent Component Analysis; the general linear instantaneous case, with mixtures possibly noisy and under-determined (number of sensors  $\leq$  number of sources) is challenging. A

common approach in such situations is sparsity-based Blind Source Separation (BSS), especially for under-determined mixtures. The basic premise is to exploit source sparsity: only a few expansion coefficients of sources are significantly different from zero. For example, recommendations in the literature include Student's  $t$  or Jeffreys' prior on  $\mathbf{s}$  (Févotte et al., 2004; Févotte and Godsill, 2006) or Laplace (Asaba et al., 2018), all of which are (or can be written as) Gaussian scale mixtures. We take a Bayesian shrinkage approach: the prior  $\mathbf{s} \sim p(\mathbf{s})$  acts as a regularization penalty and allows us to unify existing procedures as MAP estimators.

### 3.1 MacKay source distribution: hyperbolic secant

MacKay (1996) shows that the choice  $\phi_i(a_i) = -\tanh(a_i)$  is equivalent to a source distribution of the form

$$p_i(s_i) \propto \frac{1}{\cosh(s_i)} = \frac{1}{e^{s_i} + e^{-s_i}},$$

the (unstandardized) hyperbolic secant distribution. This can be written as a normal scale mixture using a Pólya-Gamma mixing density:

$$s \mid \tau \sim \mathcal{N}\left(0, \frac{1}{4\tau}\right), \quad \tau \sim PG(1, 0), \quad (4)$$

since there exists a density  $p(\tau)$  on  $\mathbb{R}^+$  such that

$$\frac{1}{\cosh(s)} \propto \int_0^\infty \exp(-2\tau s^2) p(\tau) d\tau. \quad (5)$$

Therefore, the location parameter  $s$  is a normal scale mixture, and we can further introduce a global scale  $v$  if desired:

$$s \mid v, \tau \sim \mathcal{N}\left(0, \frac{v^2}{4\tau}\right), \quad v \sim p(v), \quad \tau \sim PG(1, 0). \quad (6)$$

To see the connection to the Pólya-Gamma distribution more explicitly, recall that:

**Definition 2** Suppose  $\beta \geq 0$ . The Pólya-Gamma distribution  $PG(\beta)$  is defined as the density  $p_{PG}$  on  $\mathbb{R}^+$  whose Laplace transform satisfies

$$\cosh^{-\beta}\left(\sqrt{\frac{t}{2}}\right) = \int_0^\infty \exp(-tx) p_{PG}(x \mid \beta) dx.$$

Setting  $\beta = 1$  and choosing  $t$  appropriately yields the scale mixture representation for  $1/\cosh(s)$ . This is also connected to Jacobi theta distributions studied by Biane et al. (2001); Devroye (2009):  $J^*$  has a Jacobi distribution if

$$J^* \stackrel{d}{=} \frac{2}{\pi^2} \sum_{k=1}^{\infty} \frac{e_k}{(k - \frac{1}{2})^2}, \quad e_k \sim \mathcal{E}xp(1),$$

with moment generating function

$$\mathbb{E}(e^{-tJ^*}) = \frac{1}{\cosh \sqrt{2t}}.$$

The  $\cosh(\cdot)$  priors also have a connection with the popular horseshoe priors:

$$\beta_j \sim \mathcal{N}(0, \lambda_j^2 \tau^2 \sigma^2), \quad \lambda_j \sim p(\lambda_j) d\lambda_j, \quad \tau \sim p(\tau) d\tau.$$

The horseshoe prior places a standard half-Cauchy distribution over each local scale  $\lambda_j$ . This induces an unstandardized unit hyperbolic secant distribution over  $\xi_j = \log(\lambda_j)$  (see Polson and Scott, 2012b, Section 5):

$$p_{HS}(\xi_j) = \frac{1}{\pi} \frac{1}{\cosh(\xi_j)}.$$

Such log-scale shrinkage priors can unify many commonly used continuous shrinkage priors, as shown in Schmidt and Makalic (2018). This also provides a link between the non-Gaussian tail behavior needed for blind source separation and that of sparse signal extraction. A similar framework to horseshoe and optimal rates of reconstruction is an area of future research.

Other proposals include the scaled cosh prior (MacKay, 1996):  $p(s) \propto 1/\cosh^{1/\beta}(\beta s)$ , which has the interesting limiting behavior

$$p_i(s_i | \beta) \propto \begin{cases} \exp(-|s_i|) & \beta \rightarrow \infty \text{ (Bayesian Lasso)}, \\ \mathcal{N}(0, 1/\beta) & \beta \rightarrow 0 \text{ (Bayesian Ridge)}. \end{cases}$$

That is, in the limit  $\beta \rightarrow 0$  or  $\beta \rightarrow \infty$ , we recover the Lasso or its Bayesian analog (Tibshirani, 1996; Park and Casella, 2008), as noted by MacKay (1996).

### 3.2 Gibbs sampling strategies

Our main computational contribution is to exploit the Pólya-Gamma-augmented representation in (4) to derive a simple, fully conjugate Gibbs sampler for ICA under the hyperbolic secant source prior.

For concreteness, consider a noisy linear ICA model with  $N$  observations and  $d$  components:

$$\mathbf{x}_i | \mathbf{s}_i, \mathbf{A} \sim \mathcal{N}_d(\mathbf{A}\mathbf{s}_i, \sigma^2 \mathbf{I}_d), \quad i = 1, \dots, N,$$

where  $\mathbf{A} \in \mathbb{R}^{d \times d}$  is the mixing matrix and  $\mathbf{s}_i \in \mathbb{R}^d$  are the sources. Under the MacKay hyperbolic secant prior with Pólya-Gamma augmentation,

$$s_{ij} | \tau_{ij} \sim \mathcal{N}\left(0, \frac{1}{4\tau_{ij}}\right), \quad \tau_{ij} \sim PG(1, 0),$$

for  $i = 1, \dots, N$ ,  $j = 1, \dots, d$ . For the mixing matrix, we may place independent Gaussian priors on the columns,

$$\mathbf{a}_k \sim \mathcal{N}_d(\mathbf{0}, \sigma_2^2 \mathbf{I}_d), \quad k = 1, \dots, d,$$

where  $\mathbf{a}_k$  is the  $k$ -th column of  $\mathbf{A}$  and  $\sigma_2^2 > 0$  is a prior variance.

Let  $\mathbf{X} \in \mathbb{R}^{N \times d}$  collect the observations row-wise,  $\mathbf{S} \in \mathbb{R}^{N \times d}$  collect the sources, and  $\mathbf{T} \in \mathbb{R}^{N \times d}$  collect the latent Pólya-Gamma scales  $\tau_{ij}$ . The joint posterior  $p(\mathbf{S}, \mathbf{A}, \mathbf{T} | \mathbf{X})$  is then amenable to a three-block Gibbs sampler, cycling through:

**1. Update the sources  $\mathbf{S} \mid \mathbf{A}, \mathbf{T}, \mathbf{X}$ .** Conditionally on  $(\mathbf{A}, \mathbf{T})$ , the rows of  $\mathbf{S}$  are independent. For each  $i = 1, \dots, N$  let

$$\mathbf{D}_i = \text{diag}(4\tau_{i1}, \dots, 4\tau_{id}), \quad \Sigma_{s,i} = \left(\sigma^{-2}\mathbf{A}^\top\mathbf{A} + \mathbf{D}_i\right)^{-1},$$

and

$$\boldsymbol{\mu}_{s,i} = \sigma^{-2}\Sigma_{s,i}\mathbf{A}^\top\mathbf{x}_i.$$

Then

$$\mathbf{s}_i \mid \mathbf{A}, \mathbf{T}, \mathbf{X} \sim \mathcal{N}_d(\boldsymbol{\mu}_{s,i}, \Sigma_{s,i}).$$

**2. Update the mixing matrix  $\mathbf{A} \mid \mathbf{S}, \mathbf{X}$ .** Given  $\mathbf{S}$ , the columns of  $\mathbf{A}$  are conditionally independent. For  $k = 1, \dots, d$ , consider the  $k$ -th column of  $\mathbf{X}$ ,  $\mathbf{x}_{\cdot k} \in \mathbb{R}^N$ , and write

$$\mathbf{x}_{\cdot k} = \mathbf{S}\mathbf{a}_k + \boldsymbol{\varepsilon}_{\cdot k}, \quad \boldsymbol{\varepsilon}_{\cdot k} \sim \mathcal{N}_N(\mathbf{0}, \sigma^2\mathbf{I}_N).$$

Combining this likelihood with the Gaussian prior yields the full conditional

$$\Sigma_a = \left(\sigma^{-2}\mathbf{S}^\top\mathbf{S} + \sigma_2^{-2}\mathbf{I}_d\right)^{-1}, \quad \boldsymbol{\mu}_{a,k} = \sigma^{-2}\Sigma_a\mathbf{S}^\top\mathbf{x}_{\cdot k},$$

so that

$$\mathbf{a}_k \mid \mathbf{S}, \mathbf{X} \sim \mathcal{N}_d(\boldsymbol{\mu}_{a,k}, \Sigma_a), \quad k = 1, \dots, d.$$

**3. Update the latent Pólya-Gamma scales  $\mathbf{T} \mid \mathbf{S}$ .** Conditionally on  $\mathbf{S}$ , the entries  $\tau_{ij}$  are independent and follow Pólya-Gamma full conditionals:

$$\tau_{ij} \mid \mathbf{S}, \mathbf{X}, \mathbf{A} \sim PG(1, |2s_{ij}|), \quad i = 1, \dots, N, j = 1, \dots, d.$$

Putting these steps together, the Gibbs sampler iteratively updates

$$(\mathbf{S}^{(m)}, \mathbf{A}^{(m)}, \mathbf{T}^{(m)}) \longrightarrow (\mathbf{S}^{(m+1)}, \mathbf{A}^{(m+1)}, \mathbf{T}^{(m+1)})$$

by drawing successively from the three full conditionals above. This Pólya-Gamma-augmented Gibbs scheme is the core of our proposed Gibbs-ICE algorithm and is our main computational contribution: it yields a simple, fully conjugate MCMC method for ICA under a principled hyperbolic secant or horseshoe-type prior, while retaining exact Bayesian updating. The algorithmic steps are outlined in Algorithm 1.

**Jeffreys prior.** For completeness, we briefly recall the Jeffreys prior used in Févotte and Godsill (2006). This corresponds to the improper source distribution  $p(s) \propto 1/|s|$ . Févotte and Godsill (2006) derive an EM algorithm for MAP estimation under Jeffreys' prior using the following Normal scale mixture representation:

$$\frac{1}{|s_{ik}|} = \int \mathcal{N}(s_{ik} \mid 0, v_{ik}) \frac{1}{v_{ik}} dv_{ik}.$$

The prior  $p(v_{ik}) \propto 1/v_{ik}$  can be viewed as a limiting case of the inverse-gamma prior as both parameters approach zero, since  $p(v) \propto v^{-(a+1)}e^{b/v} \rightarrow 1/v$  as  $a, b \rightarrow 0$ . It then follows that the prior  $p(s_{ik}) \propto 1/|s_{ik}|$  can be derived as a limiting case of the  $t$ -prior in Févotte et al. (2004).

**Student's  $t$  prior (Févotte et al., 2004).** In the presence of noise,  $\mathbf{x}_j = \mathbf{A}\mathbf{s}_j + \boldsymbol{\varepsilon}_j$ ,  $j = 1, \dots, N$ , we still obtain a Gaussian scale mixture framework and EM or Gibbs algorithms can be constructed. For example, Févotte et al. (2004) provide MCMC algorithms by iterating the conditionals where each  $s_i$  has a  $t(\alpha_i, \lambda_i)$  prior with degrees of freedom  $\alpha_i$  and scale  $\lambda_i$ , which can be written as a Normal scale mixture of inverse-gamma distributions:

$$p(s_{ij} | v_{ij}) = \mathcal{N}(s_{ij} | 0, v_{ij}), \quad p(v_{ij} | \alpha_i, \lambda_i) = \mathcal{IG}\left(v_{ij} \mid \frac{\alpha_i}{2}, \frac{2}{\alpha_i \lambda_i^2}\right).$$

The resulting Gibbs sampler iterates over:

- Source update: letting  $\Sigma_{s_j} = (\sigma^{-2} \mathbf{A}^\top \mathbf{A} + \text{diag}(v_j)^{-1})^{-1}$  and  $\boldsymbol{\mu}_{s_j} = \sigma^{-2} \Sigma_{s_j} \mathbf{A}^\top \mathbf{x}_j$ ,
$$\mathbf{s}_j | \mathbf{A}, \sigma, \mathbf{v}, \boldsymbol{\alpha}, \boldsymbol{\lambda} \sim \mathcal{N}(\mathbf{s}_j | \boldsymbol{\mu}_{s_j}, \Sigma_{s_j}), \quad j = 1, \dots, N.$$
- Mixing matrix update (with Gaussian prior on  $\mathbf{A}$ ): letting  $\Sigma_a = \sigma^2 (\sum_{j=1}^N \mathbf{s}_j \mathbf{s}_j^\top)^{-1}$  and  $\boldsymbol{\mu}_a = \sigma^{-2} \Sigma_a \sum_j \mathbf{s}_j \mathbf{x}_j^\top$ ,
$$\mathbf{A} | \mathbf{S}, \sigma, \mathbf{v}, \boldsymbol{\alpha}, \boldsymbol{\lambda} \sim \mathcal{N}(\mathbf{A} | \boldsymbol{\mu}_a, \Sigma_a).$$
- Noise variance update: with  $\gamma_\sigma = dN/2$  and  $\beta_\sigma = 2 / \sum_j \|\mathbf{x}_j - \mathbf{A}\mathbf{s}_j\|_2^2$ ,
$$\sigma \sim \sqrt{\mathcal{IG}(\gamma_\sigma, \beta_\sigma)}.$$
- Local scale update: let  $\gamma_{v_i} = (\alpha_i + 1)/2$  and  $\beta_{v_i, j} = 2/(s_{ij}^2 + \alpha_i \lambda_i^2)$ , then
$$v_{ij} | \mathbf{S}, \boldsymbol{\alpha}, \boldsymbol{\lambda} \sim \mathcal{IG}(v_{ij} | \gamma_{v_i}, \beta_{v_i, j}).$$
- Hyperparameter updates for  $\lambda_i$  (and possibly  $\alpha_i$ ) from suitable gamma or other priors; see Févotte et al. (2004) for details.

**Other source distributions.** There have been a number of other source distributions analyzed in the literature. For example, finite mixtures of the form

$$p(\mathbf{s}) = \prod_{i=1}^S \sum_{\ell=1}^{M_i} p(s_i^{(\ell)}) p(\lambda_i = \ell),$$

with  $p(\lambda_i) \sim \text{Gamma}(r, c)$ , appear in constrained EM algorithms for ICA (Hinton et al., 2001). All these examples fit into the same overarching Gaussian scale mixture picture. Our focus in this paper is on the Pólya-Gamma-augmented hyperbolic secantor horseshoe-type prior, for which the Gibbs sampler above yields a particularly clean and scalable Bayesian ICA algorithm.

---

**Algorithm 1:** Pólya-Gamma-augmented Gibbs sampler for Bayesian ICA (Gibbs-ICE)

---

**Input:** Data matrix  $\mathbf{X} \in \mathbb{R}^{N \times d}$ , iterations  $M$ , noise variance  $\sigma^2$ , prior variance  $\sigma_2^2$   
**Output:** Posterior samples  $\{(\mathbf{S}^{(m)}, \mathbf{A}^{(m)}, \mathbf{T}^{(m)})\}_{m=1}^M$

**Model:**

- $\mathbf{x}_i | \mathbf{s}_i, \mathbf{A} \sim \mathcal{N}_d(\mathbf{A}\mathbf{s}_i, \sigma^2 \mathbf{I}_d), i = 1, \dots, N.$
- $s_{ij} | \tau_{ij} \sim \mathcal{N}\left(0, \frac{1}{4\tau_{ij}}\right), \tau_{ij} \sim PG(1, 0), i = 1, \dots, N, j = 1, \dots, d.$
- $\mathbf{a}_k \sim \mathcal{N}_d(\mathbf{0}, \sigma_2^2 \mathbf{I}_d), k = 1, \dots, d.$

Initialize  $\mathbf{S}^{(0)}, \mathbf{A}^{(0)}, \mathbf{T}^{(0)}$ .

**for**  $m = 1, \dots, M$  **do**

// (1) Update sources  $\mathbf{S}$   
**for**  $i = 1, \dots, N$  **do**  
 Set  $\mathbf{D}_i^{(m-1)} = \text{diag}(4\tau_{i1}^{(m-1)}, \dots, 4\tau_{id}^{(m-1)})$   
 Compute  

$$\boldsymbol{\Sigma}_{s,i}^{(m)} = \left(\sigma^{-2}(\mathbf{A}^{(m-1)})^\top \mathbf{A}^{(m-1)} + \mathbf{D}_i^{(m-1)}\right)^{-1}, \quad \boldsymbol{\mu}_{s,i}^{(m)} = \sigma^{-2} \boldsymbol{\Sigma}_{s,i}^{(m)} (\mathbf{A}^{(m-1)})^\top \mathbf{x}_i.$$
  
 Draw  $\mathbf{s}_i^{(m)} \sim \mathcal{N}_d(\boldsymbol{\mu}_{s,i}^{(m)}, \boldsymbol{\Sigma}_{s,i}^{(m)})$ .

Collect rows into  $\mathbf{S}^{(m)} = (\mathbf{s}_1^{(m)}, \dots, \mathbf{s}_N^{(m)})^\top$ .

// (2) Update mixing matrix  $\mathbf{A}$

Compute

$$\boldsymbol{\Sigma}_a^{(m)} = \left(\sigma^{-2}(\mathbf{S}^{(m)})^\top \mathbf{S}^{(m)} + \sigma_2^{-2} \mathbf{I}_d\right)^{-1}.$$

**for**  $k = 1, \dots, d$  **do**

Let  $\mathbf{x}_{\cdot k}$  be the  $k$ -th column of  $\mathbf{X}$ .  
 Set  $\boldsymbol{\mu}_{a,k}^{(m)} = \sigma^{-2} \boldsymbol{\Sigma}_a^{(m)} (\mathbf{S}^{(m)})^\top \mathbf{x}_{\cdot k}$ .  
 Draw  $\mathbf{a}_k^{(m)} \sim \mathcal{N}_d(\boldsymbol{\mu}_{a,k}^{(m)}, \boldsymbol{\Sigma}_a^{(m)})$ .

Collect columns into  $\mathbf{A}^{(m)} = (\mathbf{a}_1^{(m)}, \dots, \mathbf{a}_d^{(m)})$ .

// (3) Update Pólya-Gamma scales  $\mathbf{T}$

**for**  $i = 1, \dots, N$  **do**

**for**  $j = 1, \dots, d$  **do**

Draw  $\tau_{ij}^{(m)} \sim PG(1, |2s_{ij}^{(m)}|)$ .

## 4 Theoretical results

Early Bayesian treatments of ICA used approximate inference owing to intractable posterior computation. For instance, Attias (1999)'s Independent Factor Analysis (IFA) presents a

fully probabilistic ICA model with a flexible mixture of Gaussians prior on the sources and derives a variational EM algorithm for posterior inference. Several others adopted variational Bayes for ICA (e.g. [Lappalainen \(1999\)](#); [Choudrey and Roberts \(2003\)](#)), attesting to the popularity of the approach. Though variational and mean-field methods develop efficient approximate inference schemes, they provide no guarantees on posterior concentration or the frequentist optimality of the Bayes estimator. Similarly, [Eloyan and Ghosh \(2013\)](#), [Hyvärinen and Raju \(2002\)](#) and related work use Bayesian formulations to encode sparsity or sign constraints on the mixing matrix, motivated by EEG and neural data, but focus mostly on computation and empirical performance, not asymptotics.

### Posterior Contraction for the Unmixing Matrix with Known Source Densities

In this work, we focus on the theoretical posterior contraction behavior for the ICA unmixing matrix under the simplifying assumption that the source distributions are known. Firstly, the known-source case serves as a simple benchmark, as it eliminates the complexity of simultaneously learning the source density shapes and allows us to isolate how well the Bayesian posterior learns the unmixing matrix  $\mathbf{W}$  itself. If the posterior for the unmixing matrix can be shown to concentrate around the truth in this ideal scenario, it provides a baseline assurance that the Bayesian approach works under favorable conditions. Secondly, analyzing this case lays important groundwork for theoretical development in the realm of Bayesian ICA.

The only general posterior contraction result we are aware of is due to [Shen et al. \(2016\)](#), who study a nonparametric Bayesian block-ICA model. They place priors on (i) the unknown block partition of the sources, (ii) the mixing matrix, and (iii) the blockwise source densities using either random series or Dirichlet mixture priors. Under suitable identifiability and regularity conditions, they establish that the posterior for the joint density  $p$  of the latent sources contracts around the truth  $p_0$  (up to scale and permutation) at a minimax-optimal rate in Hellinger distance. For classical ICA without block structure, their rate reduces to  $N^{-\alpha^*/(2\alpha^*+1)}$  (up to logarithmic factors), where  $\alpha^*$  is the worst marginal smoothness, matching the 1D nonparametric density rate. Their procedure is also adaptive to the unknown smoothness and, in the block-ICA case, to the unknown block structure. However, their analysis is purely on the density level and it does not provide a  $\sqrt{N}$  asymptotic normality result for the unmixing matrix itself.

Our theoretical contribution is complementary to the rate-adaptive density results of [Shen et al. \(2016\)](#). Whereas [Shen et al. \(2016\)](#) treat both the mixing matrix  $\mathbf{A} = \mathbf{W}^{-1}$  and the blockwise source densities as unknown and derive minimax-optimal contraction rates for the joint density of the latent sources, we assume the marginal source densities  $p_{0,k}$  are known and focus on the *parametric* component of the ICA model, namely the unmixing matrix  $\mathbf{W}$ . This allows us to work in a local parametric neighborhood of  $\mathbf{W}_0$ , construct a uniform LAN expansion similar to [Vaart \(1998, Theorem 7.2\)](#), and prove that the posterior for  $\theta = \text{vec}(\mathbf{W})$  contracts at the parametric rate  $N^{-1/2}$  and satisfies a Bernstein-von Mises theorem. In particular, we obtain asymptotic normality of the posterior for  $\mathbf{W}$  up to signed permutations, something that is not covered by the analysis of [Shen et al. \(2016\)](#). Our identifiability and loss function are also different: we work with the signed-permutation distance  $d_{\pm}$  on  $\text{GL}(d)$  and show that  $d_{\pm}$  is locally equivalent to the Frobenius norm in a

neighborhood of the canonical representative  $\mathbf{W}_0$  (see Lemma 8), so that the posterior  $\sqrt{N}$  concentration in  $\theta$  translates directly to  $\sqrt{N}$  posterior concentration in  $d_{\pm}$ .

**Model and prior assumptions.** Let  $\mathbf{x}^{(1)}, \dots, \mathbf{x}^{(N)} \in \mathbb{R}^d$  be i.i.d. observations from the Independent Component Analysis (ICA) model with density

$$p_{\mathbf{W}}(x) = |\det(\mathbf{W})| \prod_{k=1}^d p_{0,k}(\mathbf{w}_k^\top x), \quad \mathbf{W} \in \mathcal{W},$$

where  $\mathbf{w}_k^\top$  denotes the  $k$ th row of the unmixing matrix  $\mathbf{W}$ , the  $p_{0,k}$  are the true source densities, and the parameter space  $\mathcal{W}$  is an open subset of the general linear group  $\text{GL}(d)$ . We endow  $\mathbf{W}$  with a prior  $\Pi$  that has a continuous and strictly positive density with respect to the Lebesgue measure on  $\text{GL}(d)$  in a neighborhood of  $\mathbf{W}_0$ . To measure the distance between an estimate  $\mathbf{W}$  and the true class around  $\mathbf{W}_0$ , we define

$$d_{\pm}(\mathbf{W}, \mathbf{W}_0) = \inf_{D, P} \|\mathbf{W} - DP\mathbf{W}_0\|_F,$$

where  $\|\cdot\|_F$  is the Frobenius norm and the infimum is taken over all signed permutation matrices  $DP$  (with  $D$  diagonal with  $\pm 1$  entries and  $P$  a permutation matrix). This distance is natural because  $\mathbf{W}_0$  is only identifiable up to signed permutations; distances between the raw matrices can be misleading, as two equally good solutions may differ by row permutations and sign flips.

We impose the following regularity and identifiability assumptions on the source densities  $p_{0,k}$ .

- (A1) **Smoothness and tails:**  $p_{0,k}$  is strictly positive and three times continuously differentiable on  $\mathbb{R}$ . The score function  $\psi_k(s) = \frac{d}{ds} \log p_{0,k}(s)$  satisfies  $\lim_{|s| \rightarrow \infty} s p_{0,k}(s) = 0$ .
- (A2) **Moment conditions:** The source random variable  $S_k \sim p_{0,k}$  satisfies  $\mathbb{E}(S_k) = 0$  and  $\text{Var}(S_k) = 1$ . The score and its derivatives satisfy  $\mathbb{E}\{\psi_k(S_k)^2\} < \infty$  and  $\mathbb{E}\{|\psi_k'(S_k)|\} < \infty$ .
- (A3) **Identifiability:** At most one source  $p_{0,k}$  is Gaussian. For every non-Gaussian source, the Fisher information for location  $J_k = \mathbb{E}\{\psi_k(S_k)^2\}$  is finite and positive. We also require non-singular Fisher information for the unmixing matrix,  $I(\mathbf{W}_0) \succ 0$ .
- (A4) **LAN regularity:** For the Local Asymptotic Normality (LAN) expansion to hold, we require, for some  $\delta > 0$ , that the third derivative of the log-density is bounded in expectation:

$$\mathbb{E} \left[ \sup_{|u| \leq \delta} |\psi_k''(S_k + u)| \right] < \infty \quad \text{and} \quad \mathbb{E}[|S_k|^3] < \infty.$$

Additionally, we need a *uniform domination* condition: there exists  $\delta > 0$  and integrable envelopes  $G_{1k}, G_{2k}$  with  $\mathbb{E}\{G_{1k}(S_k)\} < \infty$  and  $\mathbb{E}\{G_{2k}(S_k)\|\mathbf{S}\|^3\} < \infty$  (where  $\mathbf{S} = (S_1, \dots, S_d)$ ) such that

$$\sup_{|u| \leq \delta} |\psi_k'(S_k + u)| \leq G_{1k}(S_k), \quad \sup_{|u| \leq \delta} |\psi_k''(S_k + u)| \leq G_{2k}(S_k).$$

The  $C^3$  regularity of  $\log p_{0,k}$  and the integrability of the score and its derivatives in (A1)–(A2) ensure (i) differentiability under the integral sign, (ii) finite Fisher information  $J_k = \mathbb{E}\{\psi_k(S_k)^2\}$  for the sources, and (iii) the uniform third-order bounds used in Lemma 6. Light moment conditions like  $\mathbb{E}|S_k|^3 < \infty$  are standard in parametric LAN analyses; see, e.g., Vaart (1998, Ch. 7) and Miller (2021). The “at most one Gaussian” condition in (A3) is the classical ICA identifiability guarantee (Comon, 1994; Hyvärinen et al., 2001). The non-singularity of the Fisher information for  $\mathbf{W}$  at  $\mathbf{W}_0$  is the standard curvature condition for BvM. The envelopes  $G_{1k}, G_{2k}$  in (A4) provide a dominated convergence handle for the second and third derivatives of  $\log p_{0,k}$  along the local paths  $\mathbf{W}_0 + t\Delta$ . This is a routine strengthening needed to obtain *uniform* LAN on growing neighborhoods; similar domination assumptions appear in parametric BvM proofs with matrix parameters, cf. Vaart (1998, Sec. 2.3) and Kleijn and van der Vaart (2012).

Next, we impose the following prior thickness and regularity condition near  $\mathbf{W}_0$ .

(P1) **Prior thickness:** There exist  $\varepsilon_0 > 0$  and constants  $0 < c_1 \leq c_2 < \infty$  such that the prior  $\Pi$  admits a density  $\pi$  with respect to the Lebesgue measure on  $\mathcal{W}$  and

$$c_1 \leq \pi(\mathbf{W}) \leq c_2 \quad \text{for all } \mathbf{W} \text{ with } d_{\pm}(\mathbf{W}, \mathbf{W}_0) < \varepsilon_0,$$

and  $\pi$  is continuous at  $\mathbf{W}_0$ .

In the  $GL(d)$  case,  $\Pi$  assigns no mass to singular matrices and has locally integrable tails. A continuous, strictly positive prior density on a neighborhood of  $\mathbf{W}_0$  is the minimal thickness assumption in (P1) ensuring local flatness at  $N^{-1/2}$  scales, which does not necessitate specific tails or global behavior in the parametric case (Castillo and Nickl, 2013). Our choice of horseshoe-type priors slots in here, although their heavy-tailed nature is not needed specifically to prove contraction.

**Theorem 3 (Posterior contraction and Bernstein-von Mises theorem for ICA)** *Under the ICA model and assumptions (A1)–(A4) and (P1), the posterior distribution for the unmixing matrix  $\mathbf{W}$  concentrates at the parametric rate around the true signed-permutation class of  $\mathbf{W}_0$ . For any sequence  $M_N \rightarrow \infty$ ,*

$$\Pi\left(d_{\pm}(\mathbf{W}, \mathbf{W}_0) > \frac{M_N}{\sqrt{N}} \mid \mathbf{x}^{(1)}, \dots, \mathbf{x}^{(N)}\right) \xrightarrow{P_0} 0,$$

where the convergence is in probability under the true data-generating process  $P_0$ .

Moreover, the posterior distribution is asymptotically Gaussian in the following sense: let  $I(\mathbf{W}_0)$  be the Fisher information matrix of the model at  $\mathbf{W}_0$ . The posterior for the vectorized matrix  $\text{vec}(\mathbf{W})$  satisfies a Bernstein-von Mises limit:

$$\left\| \Pi\left(\sqrt{N}\{\text{vec}(\mathbf{W}) - \text{vec}(\mathbf{W}_0)\} \in \cdot \mid \mathbf{x}^{(1:N)}\right) - \mathcal{N}(\Delta_N, I(\mathbf{W}_0)^{-1}) \right\|_{\text{TV}} \xrightarrow{P_0} 0,$$

where  $\Delta_N$  is an efficient estimator, such as the MLE, centered at the true value.

A sketch of the proof of Theorem 3 follows the standard LAN-based route for finite-dimensional parametric Bayes procedures in Miller (2021); Bickel and Kleijn (2012). The key ingredient in proving Theorem 3 is the following Uniform Local Asymptotic Normality (ULAN) lemma, which gives a quadratic expansion of the log-likelihood around the true parameter  $\theta_0$  for local perturbations  $h$  in a fixed ball.

**Lemma 4 (Uniform Local Asymptotic Normality)** *Let  $\theta = \text{vec}(\mathbf{W}) \in \mathbb{R}^{d^2}$ ,  $\theta_0 = \text{vec}(\mathbf{W}_0)$ , and  $h = \sqrt{N}(\theta - \theta_0)$ . Define the per-sample log-likelihood  $\ell(\mathbf{W}; \mathbf{x}) = \log p_{\mathbf{W}}(\mathbf{x})$  and the total log-likelihood*

$$L_N(\theta) = \sum_{n=1}^N \ell(\mathbf{W}(\theta); \mathbf{x}^{(n)}),$$

where  $\mathbf{W}(\theta)$  denotes the  $d \times d$  matrix obtained by reshaping  $\theta$ . Under (A1)–(A4), for any fixed  $R > 0$ ,

$$\sup_{\|h\| \leq R} \left| L_N(\theta_0 + h/\sqrt{N}) - L_N(\theta_0) - h^\top S_N + \frac{1}{2}h^\top \mathcal{I}h \right| \xrightarrow{P_0} 0,$$

where

$$S_N := \frac{1}{\sqrt{N}} \sum_{n=1}^N \nabla_{\theta} \ell(\mathbf{W}_0; \mathbf{x}^{(n)}) \Rightarrow \mathcal{N}(0, \mathcal{I}),$$

and  $\mathcal{I} = -\mathbb{E}[\nabla_{\theta}^2 \ell(\mathbf{W}_0; X)] = I(\mathbf{W}_0)$  is the per-observation Fisher information.

The proof of Lemma 4 itself is built from three pieces: (i) the integration-by-parts identities in Lemma 5, which show that the score has mean zero and identify the information matrix; (ii) the third-order Taylor remainder bound in Lemma 6, which uses the envelope conditions in (A4) to control  $D^3 \ell(\mathbf{W}; X)$  uniformly along local paths  $\mathbf{W}_0 + t\Delta$ ; and (iii) LLNs for the Hessian to ensure  $-N^{-1} \nabla_{\theta}^2 L_N(\theta_0) \rightarrow \mathcal{I}$ . Assumption (P1) is then used in Lemma 7 to show the prior is locally flat on the  $N^{-1/2}$  scale, so the posterior kernel in the  $h$ -parametrization is essentially

$$q_N(h) \propto \exp\left(h^\top S_N - \frac{1}{2}h^\top \mathcal{I}h + r_N(h)\right),$$

up to a constant factor  $\pi(\mathbf{W}_0)$ . Lemma 9 compares the normalizing constant  $Z_N = \int q_N(h) dh$  to the Gaussian normalizer  $Z_N^0$ , showing  $Z_N/(\pi(\mathbf{W}_0)Z_N^0) \rightarrow 1$  in  $P_0$ -probability. This yields that the posterior for  $h$  is asymptotically close in total variation to  $\mathcal{N}(\mathcal{I}^{-1}S_N, \mathcal{I}^{-1})$ ; the BvM part of Theorem 3 is just this statement rewritten in terms of  $\theta = \text{vec}(\mathbf{W})$ . Finally, for the contraction part, one uses the same quadratic bound on the exponent to show that the posterior mass outside balls  $\{\|h\| \leq M_N\}$  with  $M_N \rightarrow \infty$  vanishes, and then invokes the local equivalence between  $d_{\pm}(\mathbf{W}, \mathbf{W}_0)$  and the Euclidean norm  $\|\theta - \theta_0\|$  from Lemma 8. Together, these steps establish both  $\sqrt{N}$  contraction in the identified metric  $d_{\pm}$  and the Bernstein–von Mises limit.

**On the choice and growth of  $M_N$ .** Theorem 3 is stated with an arbitrary divergent sequence  $M_N \rightarrow \infty$ . In practice one may take  $M_N = \log \log N$ , or  $M_N = (\log N)^{\alpha}$  with  $\alpha > 0$ . The proof only requires that the LAN remainder and uniform Hessian LLN hold on balls of radius  $R_N$  with  $M_N = o(R_N)$  (we use  $R_N = N^{1/6-\eta}$ ). The rate  $1/\sqrt{N}$  is sharp (parametric), and  $M_N$  simply modulates how far into the tails we ask the posterior mass to vanish.

## 5 Applications

### 5.1 Numerical Experiments

We begin with a small, controlled experiment to verify that our Gibbs sampler recovers sources and loadings under a generative model consistent with our augmentation. Throughout this subsection we fix  $n = 500$  observations and  $d = 4$  components, and generate data according to

$$\begin{aligned} \mathbf{V} &\sim \mathcal{N}_{d \times d}(\mathbf{0}, \sigma_2^2 I_d), \\ \tau_{ij} &\stackrel{\text{iid}}{\sim} \text{PG}(1, 0), \quad i = 1, \dots, n, \quad j = 1, \dots, d, \\ s_{ij} \mid \tau_{ij} &\sim \mathcal{N}(0, (4\tau_{ij})^{-1}), \\ \mathbf{x}_i \mid (\mathbf{s}_i, \mathbf{V}) &\sim \mathcal{N}_d(\mathbf{V}^\top \mathbf{s}_i, \sigma^2 I_d), \quad i = 1, \dots, n, \end{aligned} \quad (7)$$

so that  $\mathbf{X} = \mathbf{S}\mathbf{V}^\top + \boldsymbol{\varepsilon}$  with  $\boldsymbol{\varepsilon} \sim \mathcal{N}_{n \times d}(\mathbf{0}, \sigma^2 I)$ . We run our `Gibbs-ICE` sampler on  $\mathbf{X}$  and compare posterior summaries to the ground truth  $\mathbf{S}$ . For visualization, we apply a post-processing alignment that fixes permutation and sign.

**Case 1: Well-separated signals, low noise.** We set  $\sigma = 0.01$  and  $\sigma_2 = 1$ . Figure 1 overlays the marginal densities of each recovered source  $\hat{s}_{.j}$  (posterior mean) against the corresponding true  $s_{.j}$ . The Gibbs sampler closely tracks all four components: the peaks and tail thickness align well, and there is no visible mode splitting or spurious heavy-tailing. This indicates that (i) the conditional Gaussian updates for  $\mathbf{S}$  given  $\boldsymbol{\tau}$  and  $\mathbf{V}$  are numerically stable, and (ii) the overall mixing across sign and scale ambiguities has been handled adequately via alignment.

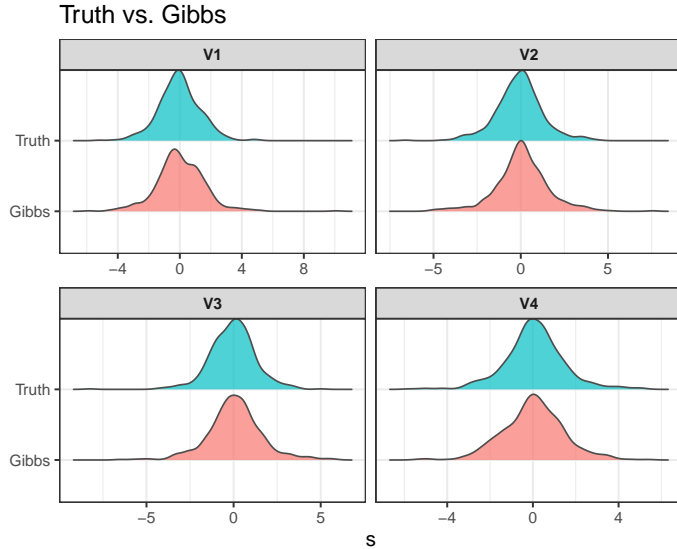


Figure 1: Posterior vs. true source densities (low noise).

**Case 2: One “hard” component and higher noise.** We increase difficulty by (a) scaling the first  $\tau_1$  by 100 times, making the first source substantially more peaked near 0, and (b) raising the observation noise to  $\sigma = 0.1$  in the data-generating process (7). Figure 2 shows the same density overlays. As expected, the first component becomes challenging: **Gibbs-ICE** still centers the mass correctly but shows attenuation near the spike and slightly broader shoulders, reflecting genuine non-identifiability introduced by a near-degenerate source convolved with higher noise. The remaining three components remain well recovered, with shapes and tail behavior close to truth.

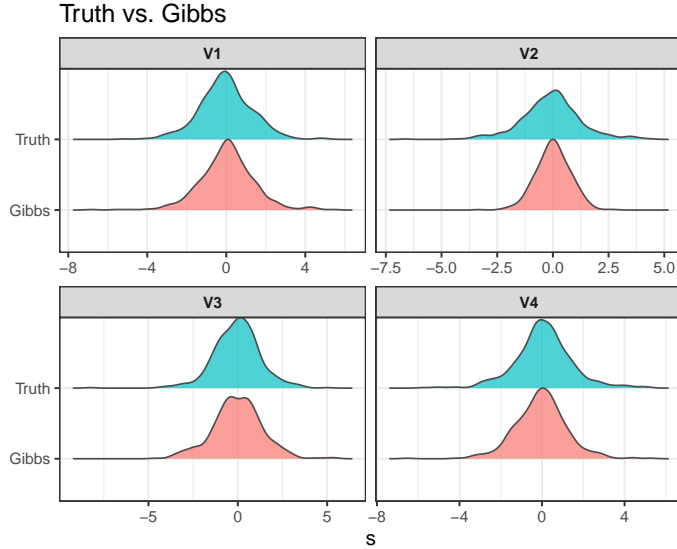


Figure 2: Posterior vs. true source densities, Case 2 (one spiky component and higher noise).

When the latent scales  $\tau$  and the noise level are benign (Case 1), **Gibbs-ICE** recovers the univariate margins of each source very closely, indicating that the conditional Pólya–Gamma blocks behave as intended. With a deliberately low variance component and higher observation noise (Case 2), the first source becomes harder, while the other components remain stable: matching intuition about ICA identifiability under super-Gaussian priors.

## 5.2 Extensive simulations against contemporary ICA methods

We benchmark **Gibbs-ICE** against widely used ICA estimators: **FastICA** (fixed-point negentropy maximization; [Hyvärinen and Oja, 2000](#)), **ProDenICA** (projection pursuit with non-parametric density estimation; [Hastie and Tibshirani, 2002a](#)), **JADE** (joint approximate diagonalization of fourth-order cumulants; [Nordhausen and Ruiz-Gazen, 2022](#)), **SOBI** (second-order blind identification via joint diagonalization of time-lagged covariances; [Belouchrani and Amin, 1998](#)), **FOBI** (fourth-order blind identification using kurtosis; [Miettinen et al., 2015](#)), **PearsonICA** (contrast based on Pearson divergences; [Karvanen and Koivunen, 2002](#)), and **steadyICA** (stable  $M$ -estimators with robust scatter; [Matteson and Tsay, 2013](#)). Un-

less stated otherwise, competing methods receive the same centered or whitened inputs and use their default contrast functions.

**Evaluation metrics.** Because ICA is identifiable only up to permutation and sign, we first align estimated sources  $\hat{\mathbf{S}}$  to the truth  $\mathbf{S}$  by solving a linear assignment on absolute correlations (Hungarian algorithm; [Kuhn, 1955](#)). We then report: (i) the *Amari distance* between the estimated unmixing  $\hat{\mathbf{W}}$  and the true  $\mathbf{W}$ ,

$$d_{\text{Amari}}(\hat{\mathbf{W}}, \mathbf{W}) = \frac{1}{2(d-1)} \left[ \sum_{i=1}^d \left( \frac{\sum_j |A_{ij}|}{\max_j |A_{ij}|} - 1 \right) + \sum_{j=1}^d \left( \frac{\sum_i |A_{ij}|}{\max_i |A_{ij}|} - 1 \right) \right], \quad \mathbf{A} = \mathbf{W}^{-1} \hat{\mathbf{W}},$$

a sign- and permutation-invariant matrix error widely used in ICA ([Amari, 1983](#)); (ii) the *source recovery correlation* (SRC), defined as the mean diagonal of  $|\text{corr}(\hat{\mathbf{S}}_{\text{aligned}}, \mathbf{S})|$  after alignment; and (iii) the *reconstruction RMSE*,

$$\text{RMSE} = \frac{\|\mathbf{X} - \hat{\mathbf{S}}_{\text{aligned}} \hat{\mathbf{A}}^\top\|_F}{\sqrt{nd}}, \quad \hat{\mathbf{A}} = \hat{\mathbf{W}}^{-1}.$$

Lower Amari and RMSE and higher SRC indicate better performance.

We consider four super-Gaussian source families commonly used in ICA stress tests: (i) **sech**, (ii) **Student- $t_3$** , (iii) **Laplace**, and (iv) **mixed** (half  $t_3$ , half Laplace). For each scenario we set  $(n, d) \in \{(500, 4), (2000, 8)\}$  and noise  $\sigma \in \{0.01, 0.05\}$ , draw  $\mathbf{S}$  i.i.d. from the chosen family and  $\mathbf{X} = \mathbf{S}\mathbf{A}^\top + \boldsymbol{\varepsilon}$  with a well-conditioned random  $\mathbf{A}$  and  $\boldsymbol{\varepsilon} \sim \mathcal{N}(\mathbf{0}, \sigma^2 I)$ . All methods are run with their recommended defaults; **Gibbs-ICE** uses 4,000 iterations (first 2,000 burn-in), thinning by 5, and posterior means for summaries.

Table 1 shows that across super-Gaussian **sech** sources, **JADE** achieves the top SRC and the lowest RMSE, while **ProDenICA** attains the best (lowest) Amari distance. For heavy-tailed  $t_3$  sources, **FastICA** dominates all three metrics. With Laplace sources, **JADE** gives the best Amari, **FastICA** yields the highest SRC, and **Gibbs-ICE** delivers the best reconstruction error (lowest RMSE), indicating strong mixing-matrix recovery up to permutation. In the mixed family, **JADE** minimizes Amari, **FastICA** maximizes SRC, and **PearsonICA** attains the lowest RMSE, suggesting that different methods excel under different criteria and distributional regimes.

Thus, if the downstream goal emphasizes accurate reconstruction or denoising, **Gibbs-ICE** is particularly attractive, especially with super-Gaussian but not ultra heavy tails. However, if the priority is pure separation under very heavy tails, contrast-based ICA methods like **FastICA** tend to win on Amari distance or SRC.

## 6 Discussion

High dimensional feature extraction has been a central tool in many modern applications. Pattern-matching methods such as deep learning compose nonlinear maps to find features. However, nonlinear ICA is notoriously hard to learn, and recent work has combined flow-based models with ICA. We develop a unified framework for optimization and posterior simulation using auxiliary variable methods. The key device is a Gaussian scale-mixture representation of the MacKay source prior  $1/\cosh(s)$  with a Pólya-Gamma mixing density,

Table 1: Aggregate ICA performance by source family. Lower Amari/RMSE and higher SRC are better. Best in each column within a source family is bolded.

Method	Source family	Performance		
		Amari ↓	SRC ↑	RMSE ↓
FOBI	sech	2.021	0.847	3.024
JADE		1.691	<b>0.986</b>	<b>2.497</b>
SOBI		1.810	0.806	3.471
FastICA		2.005	0.960	2.777
PearsonICA		1.975	0.725	2.882
steadyICA		1.477	0.863	3.383
ProDenICA		<b>1.423</b>	0.851	2.589
Gibbs-ICA	t <sub>3</sub>	1.787	0.858	2.577
FOBI		1.530	0.872	2.251
JADE		1.397	0.988	2.396
SOBI		1.510	0.739	3.458
FastICA		<b>1.203</b>	<b>0.994</b>	<b>2.096</b>
PearsonICA		1.577	0.772	3.471
steadyICA		1.717	0.991	2.561
ProDenICA	Laplace	1.782	0.798	3.396
Gibbs-ICA		1.480	0.725	2.546
FOBI		1.549	0.895	3.145
JADE		<b>1.263</b>	0.992	3.151
SOBI		1.449	0.748	3.027
FastICA		1.693	<b>0.993</b>	3.432
PearsonICA		1.610	0.830	3.602
steadyICA	Mixed	1.595	0.864	3.520
ProDenICA		1.521	0.719	3.784
Gibbs-ICA		1.543	0.983	<b>2.444</b>
FOBI		1.536	0.882	2.420
JADE		<b>1.421</b>	0.981	2.414
SOBI		1.844	0.793	2.854
FastICA		1.854	<b>0.9973</b>	3.079
PearsonICA	Mixed	2.148	0.685	<b>1.354</b>
steadyICA		1.695	0.992	3.168
ProDenICA		1.833	0.883	2.759
Gibbs-ICA		2.129	0.740	2.217

which yields conditionally Gaussian updates for the sources and loadings. This representation makes it possible to implement a fully Bayesian blockwise Gibbs sampler (see Algorithm 1). The resulting view also connects classic contrast-based ICA to envelope optimization

outlined in Appendix B, and it links directly to the Bayesian ICA literature that employs  $t$ , Laplace, and Jeffreys type source priors through a common scale–mixture lens (MacKay, 1992a; Févotte et al., 2004).

**Toward semiparametric posterior contraction.** Beyond our parametric theory for  $W$  with known source densities, we are developing semiparametric posterior contraction results in which the unmixing matrix  $\mathbf{W}$  is finite-dimensional, but the marginal source densities are *unknown* and modeled nonparametrically. The goal is to obtain joint rates in a metric that respects ICA identifiability (e.g.,  $d_{\pm}$  for  $\mathbf{W}$  and Hellinger for the product density of the latent sources), with (i) a parametric  $\sqrt{N}$  rate for  $\mathbf{W}$  and (ii) nonparametric rates  $N^{-\alpha/(2\alpha+1)}$  (up to log factors) for the source densities, governed by their marginal smoothness  $\alpha$  as in density estimation. In this setting, horseshoe–like priors on the sources are expected to play a more pronounced role: their global–local structure enforces strong shrinkage toward sparse or near–sparse coordinates while preserving *ultra heavy tails*, which helps stabilize the estimation of  $\mathbf{W}$  by adapting to unknown tail behavior and local regularity of the source densities without hand tuned bandwidths. Technically, our analysis follows a semiparametric route: we construct score functions orthogonal to the nuisance tangent space to obtain a uniform LAN expansion for  $\mathbf{W}$ , verify prior thickness and small–ball probabilities for the source priors, and control entropy of suitable sieves for the latent densities, in the spirit of adaptive nonparametric Bayes. This analysis complements the density level contraction of Shen et al. (2016), who treat both mixing and densities as unknown, by delivering parametric inference for  $W$  and nonparametric learning of the sources within a single Bayesian procedure driven by horseshoe–type shrinkage.

## References

Shun-Ichi Amari. A foundation of information geometry. *Electronics and Communications in Japan (Part I: Communications)*, 66(6):1–10, 2025/11/13 1983. doi: <https://doi.org/10.1002/ecja.4400660602>. URL <https://doi.org/10.1002/ecja.4400660602>.

D. F. Andrews and C. L. Mallows. Scale mixtures of normal distributions. *J. Roy. Statist. Soc. Ser. B*, 36:99–102, 1974. ISSN 0035-9246.

Kai Asaba, Shota Saito, Shunsuke Horii, and Toshiyasu Matsushima. Bayesian independent component analysis under hierarchical model on independent components. In *2018 Asia-Pacific Signal and Information Processing Association Annual Summit and Conference (APSIPA ASC)*, pages 959–962. IEEE, 2018.

Hagai Attias. Independent factor analysis. *Neural computation*, 11(4):803–851, 1999.

Arnab Auddy and Ming Yuan. Large dimensional independent component analysis: Statistical optimality and computational tractability. *arXiv preprint arXiv:2303.18156*, 2023.

Arnab Auddy, Dong Xia, and Ming Yuan. Tensor methods in high dimensional data analysis: Opportunities and challenges. *arXiv preprint arXiv:2405.18412*, 2024.

Horace Barlow. Redundancy reduction revisited. *Network: computation in neural systems*, 12(3):241, 2001.

Horace B Barlow. Unsupervised learning. *Neural computation*, 1(3):295–311, 1989.

O Barndorff-Nielsen, John Kent, and Michael Sørensen. Normal variance-mean mixtures and  $z$  distributions. *International Statistical Review*, 50:145–159, 1982.

Jens Behrmann, Paul Vicol, Kuan-Chieh Wang, Roger Grosse, and Jörn-Henrik Jacobsen. Understanding and mitigating exploding inverses in invertible neural networks. In *International Conference on Artificial Intelligence and Statistics*, pages 1792–1800. PMLR, 2021.

Anthony Bell and Terrence J Sejnowski. A non-linear information maximisation algorithm that performs blind separation. *Advances in neural information processing systems*, 7, 1994.

Anthony J Bell and Terrence J Sejnowski. An information-maximization approach to blind separation and blind deconvolution. *Neural computation*, 7(6):1129–1159, 1995.

Adel Belouchrani and Moeness G. Amin. Blind source separation based on time-frequency signal representations. *IEEE Trans. Signal Process.*, 46:2888–2897, 1998. URL <https://api.semanticscholar.org/CorpusID:36789524>.

Anindya Bhadra, Jyotishka Datta, Nicholas G Polson, and Brandon Willard. Global-Local Mixtures. *arXiv preprint arXiv:1604.07487*, 2016a.

Anindya Bhadra, Jyotishka Datta, Nicholas G. Polson, and Brandon T. Willard. Default Bayesian Analysis with Global-Local Shrinkage Priors. *Biometrika (to appear)*, 2016b.

Anindya Bhadra, Jyotishka Datta, Nicholas G Polson, and Brandon Willard. Horseshoe Regularization for Feature Subset Selection. *arXiv preprint arXiv:1702.07400*, 2017.

Anindya Bhadra, Jyotishka Datta, Nicholas G Polson, Vadim Sokolov, and Jianeng Xu. Merging two cultures: Deep and statistical learning. *Wiley Interdisciplinary Reviews: Computational Statistics*, 16(2):e1647, 2024.

Aditya Bhaskara, Moses Charikar, and Aravindan Vijayaraghavan. Uniqueness of tensor decompositions with applications to polynomial identifiability. In *Conference on Learning Theory*, pages 742–778. PMLR, 2014.

Philippe Biane, Jim Pitman, and Marc Yor. Probability laws related to the jacobi theta and riemann zeta functions, and brownian excursions. *Bulletin of the American Mathematical Society*, 38(4):435–465, 2001.

P. J. Bickel and B. J. K. Kleijn. The semiparametric Bernstein–von Mises theorem. *The Annals of Statistics*, 40(1), February 2012. ISSN 0090-5364. doi: 10.1214/11-aos921. URL <http://dx.doi.org/10.1214/11-AOS921>.

Guillaume Bouchard. Efficient bounds for the softmax function and applications to approximate inference in hybrid models. In *NIPS 2007 workshop for approximate Bayesian inference in continuous/hybrid systems*, volume 6, 2007.

David R. Brillinger. A Generalized Linear Model With “Gaussian” Regressor Variables. In Peter Guttorp and David Brillinger, editors, *Selected Works of David Brillinger*, Selected Works in Probability and Statistics, pages 589–606. Springer, New York, NY, 2012. ISBN 978-1-4614-1344-8.

Alexander Camuto, Matthew Willetts, Stephen Roberts, Chris Holmes, and Tom Rainforth. Towards a theoretical understanding of the robustness of variational autoencoders. In *International Conference on Artificial Intelligence and Statistics*, pages 3565–3573. PMLR, 2021.

Bradley P Carlin and Nicholas G Polson. Inference for nonconjugate bayesian models using the gibbs sampler. *Canadian Journal of statistics*, 19(4):399–405, 1991.

Carlos M Carvalho, Nicholas G Polson, and James G Scott. The horseshoe estimator for sparse signals. *Biometrika*, 97:465–480, 2010.

Ismaël Castillo and Richard Nickl. Nonparametric Bernstein–von Mises theorems in Gaussian white noise. *The Annals of Statistics*, 41(4):1999 – 2028, 2013. doi: 10.1214/13-AOS1133. URL <https://doi.org/10.1214/13-AOS1133>.

R. A. Choudrey and S. J. Roberts. Variational mixture of bayesian independent component analyzers. *Neural Comput.*, 15(1):213–252, January 2003. ISSN 0899-7667. doi: 10.1162/089976603321043766. URL <https://doi.org/10.1162/089976603321043766>.

Pierre Comon. Independent component analysis, a new concept? *Signal processing*, 36(3):287–314, 1994.

Pierre Comon, Christian Jutten, and Jeanny Herault. Blind separation of sources, part ii: Problems statement. *Signal processing*, 24(1):11–20, 1991.

Gustavo Deco and Dragan Obradovic. *An information-theoretic approach to neural computing*. Springer Science & Business Media, 1996.

Gianluca Detommaso, Jakob Kruse, Lynton Ardizzone, Carsten Rother, Ullrich Köthe, and Robert Scheichl. Hint: Hierarchical invertible neural transport for general and sequential bayesian inference. *stat*, 1050:25, 2019.

Luc Devroye. On exact simulation algorithms for some distributions related to jacobi theta functions. *Statistics & Probability Letters*, 79(21):2251–2259, 2009.

Laurent Dinh, David Krueger, and Yoshua Bengio. Nice: Non-linear independent components estimation. *arXiv preprint arXiv:1410.8516*, 2014.

Laurent Dinh, Jascha Sohl-Dickstein, and Samy Bengio. Density estimation using real nvp. *arXiv preprint arXiv:1605.08803*, 2016.

Claire Donnat, Leonardo Tozzi, and Susan Holmes. Constrained bayesian ica for brain connectome inference. *arXiv preprint arXiv:1911.05770*, 2019.

Ani Eloyan and Sujit K. Ghosh. A semiparametric approach to source separation using independent component analysis. *Computational Statistics & Data Analysis*, 58: 383–396, 2013. doi: <https://doi.org/10.1016/j.csda.2012.09.012>. URL <https://www.sciencedirect.com/science/article/pii/S0167947312003416>.

Cédric Févotte and Simon J Godsill. Blind separation of sparse sources using jeffrey’s inverse prior and the em algorithm. In *International Conference on Independent Component Analysis and Signal Separation*, pages 593–600. Springer, 2006.

Cédric Févotte, Simon J Godsill, and Patrick J Wolfe. Bayesian approach for blind separation of underdetermined mixtures of sparse sources. In *Independent Component Analysis and Blind Signal Separation: Fifth International Conference, ICA 2004, Granada, Spain, September 22-24, 2004. Proceedings 5*, pages 398–405. Springer, 2004.

Donald Geman and Chengda Yang. Nonlinear image recovery with half-quadratic regularization. *IEEE transactions on Image Processing*, 4(7):932–946, 1995.

Trevor Hastie and Rob Tibshirani. Independent components analysis through product density estimation. In *Proceedings of the 16th International Conference on Neural Information Processing Systems, NIPS’02*, page 665–672, Cambridge, MA, USA, 2002a. MIT Press.

Trevor Hastie and Rob Tibshirani. Independent components analysis through product density estimation. *Advances in neural information processing systems*, 15, 2002b.

Jeanny Herault and Christian Jutten. Space or time adaptive signal processing by neural network models. In *AIP conference proceedings*, volume 151, pages 206–211. American Institute of Physics, 1986.

Geoffrey E Hinton, Max Welling, Yee Whye Teh, and Simon Osindero. A new view of ica. In *Proceedings of 3rd International Conference on Independent Component Analysis and Blind Signal Separation (ICA’01)*, pages 746–751, 2001.

A. Hyvärinen and E. Oja. Independent component analysis: algorithms and applications. *Neural Networks*, 13(4):411–430, 2000. doi: [https://doi.org/10.1016/S0893-6080\(00\)00026-5](https://doi.org/10.1016/S0893-6080(00)00026-5). URL <https://www.sciencedirect.com/science/article/pii/S0893608000000265>.

Aapo Hyvärinen and Petteri Pajunen. Nonlinear independent component analysis: Existence and uniqueness results. *Neural networks*, 12(3):429–439, 1999.

Aapo Hyvärinen and Karthikesh Raju. Imposing sparsity on the mixing matrix in independent component analysis. *Neurocomputing*, 49(1):151–162, 2002. doi: [https://doi.org/10.1016/S0925-2312\(02\)00512-X](https://doi.org/10.1016/S0925-2312(02)00512-X). URL <https://www.sciencedirect.com/science/article/pii/S092523120200512X>.

Aapo Hyvärinen, Juha Karhunen, and Erkki Oja. *Independent component analysis, adaptive and learning systems for signal processing, communications, and control*, volume 1. John Wiley & Sons, Inc, 2001.

Tommi S Jaakkola and Michael I Jordan. A variational approach to bayesian logistic regression models and their extensions. In *Sixth International Workshop on Artificial Intelligence and Statistics*, pages 283–294. PMLR, 1997.

Jörn-Henrik Jacobsen, Arnold Smeulders, and Edouard Oyallon. i-revnet: Deep invertible networks. *arXiv preprint arXiv:1802.07088*, 2018.

Danilo Jimenez Rezende and Shakir Mohamed. Variational inference with normalizing flows. *arXiv e-prints*, pages arXiv–1505, 2015.

Yan Karklin and Michael S Lewicki. A hierarchical bayesian model for learning nonlinear statistical regularities in nonstationary natural signals. *Neural computation*, 17(2):397–423, 2005.

Juha Karvanen and Visa Koivunen. Blind separation methods based on pearson system and its extensions. *Signal Processing*, 82(4):663–673, 2002. doi: [https://doi.org/10.1016/S0165-1684\(01\)00213-4](https://doi.org/10.1016/S0165-1684(01)00213-4). URL <https://www.sciencedirect.com/science/article/pii/S0165168401002134>.

Ilyes Khemakhem, Diederik Kingma, Ricardo Monti, and Aapo Hyvarinen. Variational autoencoders and nonlinear ica: A unifying framework. In *International Conference on Artificial Intelligence and Statistics*, pages 2207–2217. PMLR, 2020.

B. J. K. Kleijn and A. W. van der Vaart. The Bernstein-Von-Mises theorem under misspecification. *Electronic Journal of Statistics*, 6(none):354–381, 1 2012. doi: 10.1214/12-EJS675. URL <https://doi.org/10.1214/12-EJS675>.

Jakob Kruse, Gianluca Detommaso, Ullrich Köthe, and Robert Scheichl. Hint: Hierarchical invertible neural transport for density estimation and bayesian inference. In *Proceedings of the AAAI Conference on Artificial Intelligence*, volume 35, pages 8191–8199, 2021.

Joseph B Kruskal. Three-way arrays: rank and uniqueness of trilinear decompositions, with application to arithmetic complexity and statistics. *Linear algebra and its applications*, 18(2):95–138, 1977.

H. W. Kuhn. The hungarian method for the assignment problem. *Naval Research Logistics Quarterly*, 2(1-2):83–97, 2025/11/13 1955. doi: <https://doi.org/10.1002/nav.3800020109>. URL <https://doi.org/10.1002/nav.3800020109>.

H. Lappalainen. Ensemble learning for independent component analysis. In *First International Workshop on Independent Component Analysis and Blind Signal Separation (ICA '99), Aussois, France, January 11-15, 1999*, pages 7–12, 1999.

Ker-Chau Li. Sliced inverse regression for dimension reduction. *Journal of the American Statistical Association*, 86(414):316–327, 1991.

Hedibert F Lopes, Nicholas G Polson, and Carlos M Carvalho. Bayesian statistics with a smile: A resampling–sampling perspective. 2012.

David JC MacKay. Bayesian interpolation. *Neural computation*, 4(3):415–447, 1992a.

David JC MacKay. Information-based objective functions for active data selection. *Neural computation*, 4(4):590–604, 1992b.

David JC MacKay. Maximum likelihood and covariant algorithms for independent component analysis, 1996.

Edward C Malthouse. Limitations of nonlinear pca as performed with generic neural networks. *IEEE Transactions on neural networks*, 9(1):165–173, 1998.

David S. Matteson and Ruey S. Tsay. Independent component analysis via distance covariance, 2013. URL <https://arxiv.org/abs/1306.4911>.

Jari Miettinen, Sara Taskinen, Klaus Nordhausen, and Hannu Oja. Fourth moments and independent component analysis. *Statistical Science*, 30(3):372–390, 8 2015. doi: 10.1214/15-STS520. URL <https://doi.org/10.1214/15-STS520>.

Jeffrey W. Miller. Asymptotic normality, concentration, and coverage of generalized posteriors, 2021. URL <https://arxiv.org/abs/1907.09611>.

Thomas Müller, Brian McWilliams, Fabrice Rousselle, Markus Gross, and Jan Novák. Neural importance sampling. *ACM Transactions on Graphics (ToG)*, 38(5):1–19, 2019.

Prasad Naik and Chih-Ling Tsai. Partial least squares estimator for single-index models. *Journal of the Royal Statistical Society: Series B (Statistical Methodology)*, 62(4):763–771, 2000.

Klaus Nordhausen and Hannu Oja. Independent component analysis: A statistical perspective. *Wiley Interdisciplinary Reviews: Computational Statistics*, 10(5):e1440, 2018.

Klaus Nordhausen and Anne Ruiz-Gazen. On the usage of joint diagonalization in multivariate statistics. *Journal of Multivariate Analysis*, 188:104844, 2022. doi: <https://doi.org/10.1016/j.jmva.2021.104844>. URL <https://www.sciencedirect.com/science/article/pii/S0047259X21001226>.

Dragan Obradovic and Gustavo Deco. Information maximization and independent component analysis: Is there a difference? *Neural Computation*, 10(8):2085–2101, 1998.

Bruno A Olshausen and David J Field. Emergence of simple-cell receptive field properties by learning a sparse code for natural images. *Nature*, 381(6583):607–609, 1996.

Bruno A Olshausen and David J Field. Sparse coding with an overcomplete basis set: A strategy employed by v1? *Vision research*, 37(23):3311–3325, 1997.

Nobutaka Ono and Shigeki Miyabe. Auxiliary-function-based independent component analysis for super-gaussian sources. In *International Conference on Latent Variable Analysis and Signal Separation*, pages 165–172. Springer, 2010.

Jason A Palmer, Kenneth Kreutz-Delgado, and Scott Makeig. Super-gaussian mixture source model for ica. In *International Conference on Independent Component Analysis and Signal Separation*, pages 854–861. Springer, 2006.

Trevor Park and George Casella. The bayesian lasso. *Journal of the American Statistical Association*, 103(482):681–686, 2008. URL <http://amstat.tandfonline.com/doi/abs/10.1198/016214508000000337>.

Barak A Pearlmutter and Lucas C Parra. A context-sensitive generalization of ica. *Advances in neural information processing systems*, 151, 1996.

Nicholas Polson and Vadim Sokolov. Deep learning: Computational aspects. *Wiley Interdisciplinary Reviews: Computational Statistics*, 12(5):e1500, 2020.

Nicholas G Polson and Veronika Rovcková. Posterior concentration for sparse deep learning. *Advances in Neural Information Processing Systems*, 31, 2018.

Nicholas G Polson and James G Scott. On the half-Cauchy prior for a global scale parameter. *Bayesian Analysis*, 7(4):887–902, 2012a.

Nicholas G. Polson and James G. Scott. On the Half-Cauchy Prior for a Global Scale Parameter. *Bayesian Analysis*, 7(4):887–902, December 2012b. ISSN 1936-0975. doi: 10.1214/12-BA730.

Nicholas G. Polson and James G. Scott. Data augmentation for non-Gaussian regression models using variance-mean mixtures. *Biometrika*, 100(2):459–471, 2013. ISSN 00063444. doi: 10.1093/biomet/ass081.

Nicholas G Polson and James G Scott. Mixtures, envelopes and hierarchical duality. *Journal of the Royal Statistical Society. Series B*, 78:701–727, 2016.

Nicholas G Polson and Vadim Sokolov. Deep learning: A bayesian perspective. *Bayesian Analysis*, 12(4):1275–1304, 2017.

Nicholas G Polson, James G Scott, and Jesse Windle. Bayesian inference for logistic models using pólya–gamma latent variables. *Journal of the American statistical Association*, 108(504):1339–1349, 2013.

Resve A Saleh and AK Saleh. Statistical properties of the log-cosh loss function used in machine learning. *arXiv preprint arXiv:2208.04564*, 2022.

RICHARD J Samworth and Ming Yuan. Independent component analysis via nonparametric maximum likelihood estimation. *The Annals of Statistics*, 40(6):2973–3002, 2012.

Daniel F Schmidt and Enes Makalic. Log-scale shrinkage priors and adaptive bayesian global-local shrinkage estimation. *arXiv preprint arXiv:1801.02321*, 2018.

Weining Shen, Jing Ning, and Ying Yuan. Rate-adaptive Bayesian independent component analysis. *Electronic Journal of Statistics*, 10(2):3247 – 3264, 2016. doi: 10.1214/16-EJS1183. URL <https://doi.org/10.1214/16-EJS1183>.

Yang Song, Chenlin Meng, and Stefano Ermon. Mintnet: Building invertible neural networks with masked convolutions. *Advances in Neural Information Processing Systems*, 32, 2019.

R. Tibshirani. Regression Shrinkage and Selection via the Lasso. *Journal of the Royal Statistical Society. Series B*, 58:267–288, 1996.

M-N Tran, Nghia Nguyen, David Nott, and Robert Kohn. Bayesian deep net glm and glmm. *Journal of Computational and Graphical Statistics*, 29(1):97–113, 2020.

Brian L Trippe and Richard E Turner. Conditional density estimation with bayesian normalising flows. *arXiv preprint arXiv:1802.04908*, 2018.

A. W. van der Vaart. *Asymptotic Statistics*. Cambridge Series in Statistical and Probabilistic Mathematics. Cambridge University Press, Cambridge, 1998. ISBN 9780521784504. doi: DOI:10.1017/CBO9780511802256. URL <https://www.cambridge.org/core/product/A3C7DAD3F7E66A1FA60E9C8FE132EE1D>.

Yuxi Wang, Nicholas Polson, and Vadim O Sokolov. Data augmentation for bayesian deep learning. *Bayesian Analysis*, 18(4):1041–1069, 2023.

Mike West. On scale mixtures of normal distributions. *Biometrika*, 74(3):646–648, 1987.

## Appendix A. Additional Theoretical Results

We need the following identities to prove our main theoretical results.

**Lemma 5** *Under (A1)–(A2), the following identities hold:*

$$\mathbb{E}[\psi_k(S_k) S_k] = -1, \quad k = 1, \dots, d, \quad (8)$$

$$\mathbb{E}[\psi(\mathbf{S}) \mathbf{S}^\top] = -I_d, \quad (9)$$

and consequently, with  $\mathbf{A}_0 = \mathbf{W}_0^{-1}$  and  $\mathbf{X} = \mathbf{A}_0 \mathbf{S}$ ,

$$\mathbb{E} U(\mathbf{W}_0; \mathbf{X}) = (\mathbf{W}_0^{-1})^\top + \mathbb{E}[\psi(\mathbf{S}) \mathbf{X}^\top] = (\mathbf{W}_0^{-1})^\top - \mathbf{A}_0^\top = 0. \quad (10)$$

**Proof** Fix  $k \in \{1, \dots, d\}$ . By definition  $\psi_k(s) = \frac{d}{ds} \log p_{0,k}(s) = \frac{p'_{0,k}(s)}{p_{0,k}(s)}$ , so

$$\mathbb{E}[\psi_k(S_k) S_k] = \int_{\mathbb{R}} \psi_k(s) s p_{0,k}(s) ds = \int_{\mathbb{R}} s p'_{0,k}(s) ds.$$

Apply integration by parts with  $u(s) = s$  and  $dv = p'_{0,k}(s) ds$  (hence  $du = ds$  and  $v = p_{0,k}(s)$ ):

$$\int_{\mathbb{R}} s p'_{0,k}(s) ds = [s p_{0,k}(s)]_{-\infty}^{+\infty} - \int_{\mathbb{R}} p_{0,k}(s) ds.$$

Assumption (A1) gives  $\lim_{|s| \rightarrow \infty} s p_{0,k}(s) = 0$ , so the boundary term vanishes, and since  $p_{0,k}$  is a density,  $\int_{\mathbb{R}} p_{0,k}(s) ds = 1$ . Therefore (8) holds:

$$\mathbb{E}[\psi_k(S_k) S_k] = 0 - 1 = -1.$$

Next, write  $\mathbf{S} = (S_1, \dots, S_d)^\top$  with independent coordinates and joint density  $\prod_{m=1}^d p_{0,m}(s_m)$ . The  $(k, j)$  entry of  $\mathbb{E}[\psi(\mathbf{S}) \mathbf{S}^\top]$  is

$$\mathbb{E}[\psi_k(S_k) S_j] = \int_{\mathbb{R}^d} \psi_k(s_k) s_j \prod_{m=1}^d p_{0,m}(s_m) ds_1 \cdots ds_d.$$

If  $j = k$ , Fubini reduces this to the one-dimensional identity (8), giving  $\mathbb{E}[\psi_k(S_k) S_k] = -1$ . If  $j \neq k$ , independence factorizes the integral:

$$\mathbb{E}[\psi_k(S_k) S_j] = \left( \int_{\mathbb{R}} \psi_k(s_k) p_{0,k}(s_k) ds_k \right) \left( \int_{\mathbb{R}} s_j p_{0,j}(s_j) ds_j \right) = \mathbb{E}[\psi_k(S_k)] \cdot \mathbb{E}[S_j].$$

Now

$$\mathbb{E}[\psi_k(S_k)] = \int_{\mathbb{R}} \frac{p'_{0,k}(s)}{p_{0,k}(s)} p_{0,k}(s) ds = \int_{\mathbb{R}} p'_{0,k}(s) ds = [p_{0,k}(s)]_{-\infty}^{+\infty} = 0,$$

since (A1) implies  $p_{0,k}(s) \rightarrow 0$  as  $|s| \rightarrow \infty$  (indeed  $s p_{0,k}(s) \rightarrow 0$  implies  $p_{0,k}(s) = o(1/|s|)$ ). Therefore  $\mathbb{E}[\psi_k(S_k) S_j] = 0$  for  $j \neq k$ . Combining the diagonal and off-diagonal cases yields (9):

$$\mathbb{E}[\psi(\mathbf{S}) \mathbf{S}^\top] = -I_d.$$

Finally, with  $\mathbf{X} = \mathbf{A}_0 \mathbf{S}$  and  $\mathbf{A}_0 = \mathbf{W}_0^{-1}$ , compute the mean of the matrix score

$$U(\mathbf{W}_0; \mathbf{X}) = (\mathbf{W}_0^{-1})^\top + \psi(\mathbf{S}) \mathbf{X}^\top = (\mathbf{W}_0^{-1})^\top + \psi(\mathbf{S}) \mathbf{S}^\top \mathbf{A}_0^\top,$$

to obtain

$$\mathbb{E} U(\mathbf{W}_0; \mathbf{X}) = (\mathbf{W}_0^{-1})^\top + \mathbb{E}[\psi(\mathbf{S}) \mathbf{S}^\top] \mathbf{A}_0^\top = (\mathbf{W}_0^{-1})^\top - \mathbf{A}_0^\top = 0,$$

which is (10).  $\blacksquare$

**Lemma 6 (Third-order Taylor remainder)** *Let  $\theta = \text{vec}(\mathbf{W}) \in \mathbb{R}^p$ ,  $\theta_0 = \text{vec}(\mathbf{W}_0)$ , and  $h = \sqrt{N}(\theta - \theta_0)$ . Write  $\Delta := \frac{1}{\sqrt{N}} \text{mat}(h) \in \mathbb{R}^{d \times d}$  and  $\mathbf{W}_t := \mathbf{W}_0 + t\Delta$  for  $t \in [0, 1]$ . For one observation  $\mathbf{X}$ , set*

$$\ell(\mathbf{W}; \mathbf{X}) = \log |\mathbf{W}| + \sum_{k=1}^d \log p_{0,k}(\mathbf{w}_k^\top \mathbf{X}),$$

where  $\mathbf{w}_k^\top$  is the  $k$ th row of  $\mathbf{W}$ . Assume (A1)–(A4). Then for any fixed  $R > 0$ , there exists  $N_0(R)$  such that for all  $N \geq N_0(R)$ , the third-order Taylor remainder of the  $N$ -sample log-likelihood,

$$R_N(h) := \sum_{i=1}^N \int_0^1 \frac{(1-t)^2}{2} D^3 \ell(\mathbf{W}_t; \mathbf{X}^{(i)}) [\Delta, \Delta, \Delta] dt,$$

satisfies

$$\sup_{\|h\| \leq R} |R_N(h)| = O_P\left(\frac{\|h\|^3}{\sqrt{N}}\right).$$

**Proof** Throughout,  $\|\cdot\|$  denotes the Euclidean norm for vectors and the Frobenius norm for matrices;  $\|\cdot\|_{\text{op}}$  is the operator norm. Since the map  $\theta \mapsto \mathbf{W}$  is linear, there exists a constant  $c_T > 0$  such that

$$\|\Delta\| \leq \frac{c_T}{\sqrt{N}} \|h\|. \quad (11)$$

**Uniform invertibility along the path.** Fix  $R > 0$ . Because  $\mathbf{W}_0$  is nonsingular and the inversion map  $\mathbf{W} \mapsto \mathbf{W}^{-1}$  is continuous, there exists  $\eta > 0$  and a finite constant  $C_*$  such that

$$\|\mathbf{W} - \mathbf{W}_0\|_F < \eta \implies \|\mathbf{W}^{-1}\|_{\text{op}} \leq C_*.$$

Choose  $N_0(R)$  so large that  $\sup_{\|h\| \leq R} \|\Delta\| \leq \eta$  for all  $N \geq N_0(R)$ , cf. (11). Then for all  $t \in [0, 1]$ ,  $N \geq N_0(R)$  and  $\|h\| \leq R$ ,

$$\|\mathbf{W}_t^{-1}\|_{\text{op}} \leq C_* \quad \text{and hence} \quad \|\mathbf{W}_t^{-1}\|_{\text{op}}^3 \leq C_*^3. \quad (12)$$

**Third order integral remainder and decomposition.** We use the third-order integral remainder for each observation  $\mathbf{X}$ :

$$R^{(1)}(h; \mathbf{X}) := \int_0^1 \frac{(1-t)^2}{2} D^3 \ell(\mathbf{W}_t; \mathbf{X}) [\Delta, \Delta, \Delta] dt, \quad R_N(h) = \sum_{i=1}^N R^{(1)}(h; \mathbf{X}^{(i)}).$$

We bound separately the contributions from  $\log ||W|$  and from the source likelihood  $\ell_{\text{src}} = \sum_{k=1}^d \log p_{0,k}(\mathbf{w}_k^\top \mathbf{X})$ .

Matrix differential calculus yields

$$D \log ||W| [H] = \text{tr}(\mathbf{W}^{-1} H), \quad D^2 \log ||W| [H, K] = -\text{tr}(\mathbf{W}^{-1} H \mathbf{W}^{-1} K),$$

and

$$D^3 \log ||W| [H, H, H] = 2 \text{tr}(\mathbf{W}^{-1} H \mathbf{W}^{-1} H \mathbf{W}^{-1} H).$$

Hence, with  $H = \Delta$  and  $\mathbf{W} = \mathbf{W}_t$ ,

$$|D^3 \log ||W_t| [\Delta, \Delta, \Delta]| \leq 2 \|\mathbf{W}_t^{-1}\|_{\text{op}}^3 \|\Delta\|^3 \leq 2 C_*^3 \|\Delta\|^3,$$

by (12). Therefore, for each  $\mathbf{X}$ ,

$$\left| \int_0^1 \frac{(1-t)^2}{2} D^3 \log ||W_t| [\Delta, \Delta, \Delta] dt \right| \leq \frac{2 C_*^3}{2} \|\Delta\|^3 \leq \frac{C_1}{N^{3/2}} \|h\|^3$$

with  $C_1 := C_*^3 c_T^3$ . Summing over  $i = 1, \dots, N$  gives

$$\sum_{i=1}^N \left| \int_0^1 \frac{(1-t)^2}{2} D^3 \log ||W_t| [\Delta, \Delta, \Delta] dt \right| \leq N \frac{C_1}{N^{3/2}} \|h\|^3 = \frac{C_1}{\sqrt{N}} \|h\|^3. \quad (13)$$

Let  $s_k(\mathbf{W}) := \mathbf{w}_k^\top \mathbf{X}$ . Then  $Ds_k(\mathbf{W})[H] = H_k \mathbf{X}$  and  $D^2 s_k \equiv 0$ . With  $\psi_k = \partial_s \log p_{0,k}$  and  $\psi'_k, \psi''_k$  its derivatives,

$$\begin{aligned} D \left( \sum_{k=1}^d \log p_{0,k}(s_k(\mathbf{W})) \right) [H] &= \sum_{k=1}^d \psi_k(s_k(\mathbf{W})) (H_k \mathbf{X}), \\ D^2 \left( \sum_{k=1}^d \log p_{0,k}(s_k(\mathbf{W})) \right) [H, H] &= \sum_{k=1}^d \psi'_k(s_k(\mathbf{W})) (H_k \mathbf{X})^2, \\ D^3 \left( \sum_{k=1}^d \log p_{0,k}(s_k(\mathbf{W})) \right) [H, H, H] &= \sum_{k=1}^d \psi''_k(s_k(\mathbf{W})) (H_k \mathbf{X})^3. \end{aligned}$$

Therefore, at  $\mathbf{W}_t$  and  $H = \Delta$ ,

$$|D^3 \ell_{\text{src}}(\mathbf{W}_t; \mathbf{X}) [\Delta, \Delta, \Delta]| \leq \sum_{k=1}^d \sup_{u \in \mathcal{U}_{k,t}(\mathbf{X})} |\psi''_k(u)| |\Delta_k \mathbf{X}|^3, \quad (14)$$

where  $s_k(\mathbf{W}_t) = \mathbf{w}_{0,k}^\top \mathbf{X} + t \Delta_k \mathbf{X} =: S_k + t \Delta_k \mathbf{X}$ , hence

$$\mathcal{U}_{k,t}(\mathbf{X}) := \{S_k + \tau \Delta_k \mathbf{X} : \tau \in [0, 1]\}.$$

Assumption (A4) implies in particular  $\mathbb{E}G_{2k}(S_k) < \infty$  and  $\mathbb{E}\|\mathbf{X}\|^3 \sum_k G_{2k}(S_k) < \infty$  since  $\mathbf{X} = \mathbf{A}_0 \mathbf{S}$ .

Define the event

$$\mathcal{M}(\mathbf{X}) := \left\{ \max_{1 \leq k \leq d} |\Delta_k \mathbf{X}| \leq \delta \right\}.$$

On  $\mathcal{M}(\mathbf{X})$ , (A4) and (14) give

$$\sup_{t \in [0,1]} \left| D^3 \ell_{\text{src}}(\mathbf{W}_t; \mathbf{X}) [\Delta, \Delta, \Delta] \right| \leq \sum_{k=1}^d G_{2k}(S_k) |\Delta_k \mathbf{X}|^3 \leq \|\Delta\|^3 \|\mathbf{X}\|^3 \sum_{k=1}^d G_{2k}(S_k),$$

and hence

$$\int_0^1 \frac{(1-t)^2}{2} \left| D^3 \ell_{\text{src}}(\mathbf{W}_t; \mathbf{X}) [\Delta, \Delta, \Delta] \right| dt \leq \frac{1}{2} \|\Delta\|^3 \|\mathbf{X}\|^3 \sum_{k=1}^d G_{2k}(S_k). \quad (15)$$

Because  $\mathbf{X} = \mathbf{A}_0 \mathbf{S}$ ,  $\|\mathbf{X}\| \leq \|\mathbf{A}_0\|_{\text{op}} \|\mathbf{S}\|$ , and by (A4),

$$\mathbb{E} \left[ \|\mathbf{X}\|^3 \sum_{k=1}^d G_{2k}(S_k) \right] \leq \|\mathbf{A}_0\|_{\text{op}}^3 \mathbb{E} \left[ \|\mathbf{S}\|^3 \sum_{k=1}^d G_{2k}(S_k) \right] < \infty.$$

It remains to control  $\mathcal{M}(\mathbf{X})^c$ . Using  $|\Delta_k \mathbf{X}| \leq \|\Delta_k\| \|\mathbf{X}\| \leq \|\Delta\| \|\mathbf{X}\|$  and Markov's inequality,

$$\mathbb{P}(\mathcal{M}(\mathbf{X})^c) \leq \sum_{k=1}^d \mathbb{P}(|\Delta_k \mathbf{X}| > \delta) \leq \sum_{k=1}^d \frac{\mathbb{E}|\Delta_k \mathbf{X}|^3}{\delta^3} \leq \frac{d}{\delta^3} \|\Delta\|^3 \mathbb{E}\|\mathbf{X}\|^3 = O\left(\frac{\|h\|^3}{N^{3/2}}\right),$$

by (11). For i.i.d.  $\mathbf{X}^{(1)}, \dots, \mathbf{X}^{(N)}$ , a union bound gives

$$\mathbb{P}\left(\exists i \leq N : \mathcal{M}(\mathbf{X}^{(i)})^c\right) \leq N \cdot O\left(\frac{\|h\|^3}{N^{3/2}}\right) = O\left(\frac{\|h\|^3}{\sqrt{N}}\right).$$

On the complementary event (which has probability  $1 - O(\|h\|^3/\sqrt{N})$ ), applying (15) to each  $\mathbf{X}^{(i)}$  and summing yields

$$\sum_{i=1}^N \int_0^1 \frac{(1-t)^2}{2} \left| D^3 \ell_{\text{src}}(\mathbf{W}_t; \mathbf{X}^{(i)}) [\Delta, \Delta, \Delta] \right| dt \leq \frac{1}{2} \|\Delta\|^3 \sum_{i=1}^N \|\mathbf{X}^{(i)}\|^3 \sum_{k=1}^d G_{2k}(S_k^{(i)}).$$

By the strong law of large numbers and finiteness of  $\mathbb{E}[\|\mathbf{X}\|^3 \sum_k G_{2k}(S_k)]$ ,

$$\frac{1}{N} \sum_{i=1}^N \|\mathbf{X}^{(i)}\|^3 \sum_{k=1}^d G_{2k}(S_k^{(i)}) \xrightarrow{\text{a.s.}} \mathbb{E} \left[ \|\mathbf{X}\|^3 \sum_{k=1}^d G_{2k}(S_k) \right] =: C_3 < \infty.$$

Using (11), we obtain on this event

$$\sum_{i=1}^N \int_0^1 \frac{(1-t)^2}{2} \left| D^3 \ell_{\text{src}}(\mathbf{W}_t; \mathbf{X}^{(i)}) [\Delta, \Delta, \Delta] \right| dt \leq \frac{1}{2} \frac{c_T^3}{N^{3/2}} \|h\|^3 \cdot N \cdot (C_3 + o(1)) = O\left(\frac{\|h\|^3}{\sqrt{N}}\right).$$

Since the complement event has probability  $O(\|h\|^3/\sqrt{N})$  uniformly over  $\|h\| \leq R$ , the above bound implies

$$\sup_{\|h\| \leq R} \sum_{i=1}^N \int_0^1 \frac{(1-t)^2}{2} |D^3 \ell_{\text{src}}(\mathbf{W}_t; \mathbf{X}^{(i)}) [\Delta, \Delta, \Delta]| dt = O_P\left(\frac{\|h\|^3}{\sqrt{N}}\right).$$

Combining the determinant bound (13) with the source contribution just obtained yields, uniformly over  $\|h\| \leq R$ ,

$$|R_N(h)| = O_P\left(\frac{\|h\|^3}{\sqrt{N}}\right).$$

All constants above depend only on  $R$ ,  $d$ ,  $\mathbf{W}_0$  and the source distribution through the moments and envelopes in (A1)–(A4), and are independent of  $N$  and  $h$ . This completes the proof.  $\blacksquare$

**Lemma 7 (Prior thickness / local flatness)** *Under (P1), for any fixed  $R > 0$ ,*

$$\sup_{\|h\| \leq R} \left| \log \frac{\pi(\mathbf{W}(\theta_0 + h/\sqrt{N}))}{\pi(\mathbf{W}_0)} \right| \xrightarrow{P_0} 0, \quad \inf_{\|h\| \leq R} \pi(\mathbf{W}(\theta_0 + h/\sqrt{N})) \asymp \pi(\mathbf{W}_0) > 0.$$

**Proof** [Proof of Lemma 7] Fix  $R > 0$ . Write  $\theta = \text{vec}(\mathbf{W}) \in \mathbb{R}^p$  with  $p = d^2$ , and let  $\kappa : \mathbb{R}^p \rightarrow \mathbb{R}^{d \times d}$  be the inverse vectorization map. For  $h \in \mathbb{R}^p$  set

$$\mathbf{W}_N(h) := \mathbf{W}(\theta_0 + h/\sqrt{N}) = \kappa(\theta_0) + \kappa(h)/\sqrt{N} = \mathbf{W}_0 + \Delta_N(h),$$

where  $\Delta_N(h) := \kappa(h)/\sqrt{N}$ . Since  $\kappa$  is linear, there exists a constant  $c_T > 0$  (depending only on the choice of norms on  $\mathbb{R}^p$  and  $\mathbb{R}^{d \times d}$ ) such that

$$\sup_{\|h\| \leq R} \|\mathbf{W}_N(h) - \mathbf{W}_0\|_F = \sup_{\|h\| \leq R} \|\Delta_N(h)\|_F \leq \frac{c_T R}{\sqrt{N}} \xrightarrow{N \rightarrow \infty} 0. \quad (16)$$

By assumption (P1), there exist  $\varepsilon_0 > 0$  and constants  $0 < c_1 \leq c_2 < \infty$  such that

$$c_1 \leq \pi(\mathbf{W}) \leq c_2 \quad \text{for all } \mathbf{W} \text{ with } \|\mathbf{W} - \mathbf{W}_0\|_F < \varepsilon_0,$$

and  $\pi$  is continuous at  $\mathbf{W}_0$ . Because  $\pi$  is bounded away from zero on the open ball  $B(\mathbf{W}_0, \varepsilon_0)$ ,  $\log \pi$  is well-defined and continuous on  $B(\mathbf{W}_0, \varepsilon_0)$  as well.

Let  $\varepsilon > 0$  be arbitrary. By continuity of  $\pi$  and  $\log \pi$  at  $\mathbf{W}_0$ , there exists  $\delta \in (0, \varepsilon_0)$  such that

$$\|\mathbf{W} - \mathbf{W}_0\|_F < \delta \implies |\pi(\mathbf{W}) - \pi(\mathbf{W}_0)| < \varepsilon \quad \text{and} \quad |\log \pi(\mathbf{W}) - \log \pi(\mathbf{W}_0)| < \varepsilon. \quad (17)$$

By (16), choose  $N_1(\varepsilon, R)$  large enough so that  $c_T R / \sqrt{N} < \delta$  for all  $N \geq N_1$ . Then, for all such  $N$ ,

$$\sup_{\|h\| \leq R} \|\mathbf{W}_N(h) - \mathbf{W}_0\|_F < \delta,$$

and hence by (17),

$$\sup_{\|h\| \leq R} |\log \pi(\mathbf{W}_N(h)) - \log \pi(\mathbf{W}_0)| \leq \varepsilon, \quad \sup_{\|h\| \leq R} |\pi(\mathbf{W}_N(h)) - \pi(\mathbf{W}_0)| \leq \varepsilon. \quad (18)$$

The first statement in the lemma follows immediately from (18):

$$\sup_{\|h\| \leq R} \left| \log \frac{\pi(\mathbf{W}(\theta_0 + h/\sqrt{N}))}{\pi(\mathbf{W}_0)} \right| = \sup_{\|h\| \leq R} |\log \pi(\mathbf{W}_N(h)) - \log \pi(\mathbf{W}_0)| \xrightarrow{N \rightarrow \infty} 0.$$

This convergence is deterministic, hence also in  $P_0$ -probability.

For the thickness statement, (18) implies

$$\pi(\mathbf{W}_0) - \varepsilon \leq \inf_{\|h\| \leq R} \pi(\mathbf{W}(\theta_0 + h/\sqrt{N})) \leq \sup_{\|h\| \leq R} \pi(\mathbf{W}(\theta_0 + h/\sqrt{N})) \leq \pi(\mathbf{W}_0) + \varepsilon,$$

for all  $N \geq N_1(\varepsilon, R)$ . In particular, choosing  $\varepsilon \leq \pi(\mathbf{W}_0)/2$  we get

$$\inf_{\|h\| \leq R} \pi(\mathbf{W}(\theta_0 + h/\sqrt{N})) \geq \frac{\pi(\mathbf{W}_0)}{2} > 0,$$

so the infimum is bounded below by a fixed positive constant for all large  $N$ , and the values are uniformly comparable to  $\pi(\mathbf{W}_0)$ ; equivalent to  $\inf_{\|h\| \leq R} \pi(\cdot) \asymp \pi(\mathbf{W}_0) > 0$ .

This completes the proof. ■

The following result proves the local equivalence of  $d_{\pm}$  and Euclidean distance.

**Lemma 8** *Let  $\mathcal{G} := \{DP : D = \text{diag}(\pm 1, \dots, \pm 1), P \text{ permutation}\}$  be the finite signed permutation group acting on  $\mathbb{R}^{d \times d}$  by left multiplication. Fix a canonical representative  $\mathbf{W}_0$  of the signed-permutation equivalence class, chosen by a deterministic tie-breaking rule, so that the stabilizer of  $\mathbf{W}_0$  in  $\mathcal{G}$  is trivial:*

$$g\mathbf{W}_0 = \mathbf{W}_0 \implies g = I_d.$$

Define

$$d_{\pm}(\mathbf{W}, \mathbf{W}_0) := \min_{g \in \mathcal{G}} \|\mathbf{W} - g\mathbf{W}_0\|_F.$$

Then there exists  $\varepsilon > 0$  such that

$$\|\mathbf{W} - \mathbf{W}_0\|_F < \varepsilon \implies d_{\pm}(\mathbf{W}, \mathbf{W}_0) = \|\mathbf{W} - \mathbf{W}_0\|_F.$$

Consequently, in a neighborhood of  $\mathbf{W}_0$ ,  $d_{\pm}(\cdot, \mathbf{W}_0)$  is equivalent to the Frobenius distance and hence to the Euclidean distance in any linear parameterization  $\theta = \text{vec}(\mathbf{W})$ : there exist constants  $0 < c_1 \leq c_2 < \infty$  and  $\eta > 0$  such that for all  $\theta$  with  $\|\theta - \theta_0\| < \eta$ ,

$$c_1 \|\theta - \theta_0\| \leq d_{\pm}(\mathbf{W}(\theta), \mathbf{W}_0) \leq c_2 \|\theta - \theta_0\|.$$

**Proof** Because  $\mathcal{G}$  is finite and the stabilizer of  $\mathbf{W}_0$  is trivial, the set  $\{g\mathbf{W}_0 : g \in \mathcal{G}\}$  consists of  $|\mathcal{G}|$  distinct matrices. Hence the minimum pairwise distance from  $\mathbf{W}_0$  is strictly positive:

$$\delta := \min_{g \in \mathcal{G}, g \neq I_d} \|g\mathbf{W}_0 - \mathbf{W}_0\|_F > 0.$$

Let  $\varepsilon := \delta/2$ . If  $\|\mathbf{W} - \mathbf{W}_0\|_F < \varepsilon$ , then for any  $g \neq I_d$ ,

$$\|\mathbf{W} - g\mathbf{W}_0\|_F \geq \|g\mathbf{W}_0 - \mathbf{W}_0\|_F - \|\mathbf{W} - \mathbf{W}_0\|_F \geq \delta - \varepsilon = \varepsilon > \|\mathbf{W} - \mathbf{W}_0\|_F.$$

Thus the minimizer of  $g \mapsto \|\mathbf{W} - g\mathbf{W}_0\|_F$  is  $g = I_d$ , and  $d_{\pm}(\mathbf{W}, \mathbf{W}_0) = \|\mathbf{W} - \mathbf{W}_0\|_F$  whenever  $\|\mathbf{W} - \mathbf{W}_0\|_F < \varepsilon$ .

Let  $\theta = \text{vec}(\mathbf{W})$  and  $\theta_0 = \text{vec}(\mathbf{W}_0)$ . Since  $\text{vec} : \mathbb{R}^{d \times d} \rightarrow \mathbb{R}^{d^2}$  is a linear isomorphism, all norms are equivalent in finite dimension. In particular, there exist constants  $a, b \in (0, \infty)$  such that

$$a \|\theta - \theta_0\| \leq \|\mathbf{W} - \mathbf{W}_0\|_F \leq b \|\theta - \theta_0\| \quad \text{for all } \mathbf{W}.$$

Combining these inequalities gives, for all  $\|\theta - \theta_0\|$  small enough so that  $\|\mathbf{W} - \mathbf{W}_0\|_F < \varepsilon$ ,

$$a \|\theta - \theta_0\| \leq d_{\pm}(\mathbf{W}(\theta), \mathbf{W}_0) \leq b \|\theta - \theta_0\|.$$

Setting  $c_1 = a$ ,  $c_2 = b$ , and choosing  $\eta > 0$  to enforce  $\|\mathbf{W} - \mathbf{W}_0\|_F < \varepsilon$  completes the proof.  $\blacksquare$

**Proof** [Proof of Lemma 4] Write  $\mathbf{A}_0 = \mathbf{W}_0^{-1}$  and  $\mathbf{X} \stackrel{d}{=} \mathbf{A}_0 \mathbf{S}$  with independent sources  $\mathbf{S} = (S_1, \dots, S_d)^\top$ ,  $S_k \sim p_{0,k}$ . Let  $\psi_k = \partial_s \log p_{0,k}$  and  $J_k = \mathbb{E}[\psi_k(S_k)^2]$ . As before, for  $\theta = \text{vec}(\mathbf{W})$  and  $\theta_0 = \text{vec}(\mathbf{W}_0)$  set  $h = \sqrt{N}(\theta - \theta_0)$  and denote by  $\kappa : \mathbb{R}^{d^2} \rightarrow \mathbb{R}^{d \times d}$  the inverse vectorization map. Define

$$\Delta := \frac{1}{\sqrt{N}} \kappa(h), \quad \mathbf{W}_t := \mathbf{W}_0 + t \Delta, \quad t \in [0, 1].$$

Because  $\kappa$  is linear, there exists  $c_T > 0$  with  $\|\Delta\| \leq c_T \|h\|/\sqrt{N}$ .

The matrix score at  $\mathbf{W}$  can be written as

$$U(\mathbf{W}; \mathbf{X}) = (\mathbf{W}^{-1})^\top + \psi(\mathbf{S}(\mathbf{W})) \mathbf{X}^\top, \quad \mathbf{S}(\mathbf{W}) = \mathbf{W} \mathbf{X},$$

hence at  $\mathbf{W}_0$ ,

$$U(\mathbf{W}_0; \mathbf{X}) = (\mathbf{W}_0^{-1})^\top + \psi(\mathbf{S}) \mathbf{X}^\top, \quad \mathbf{X} = \mathbf{A}_0 \mathbf{S}.$$

By Lemma 5,  $\mathbb{E}U(\mathbf{W}_0; \mathbf{X}) = 0$ . Let

$$S_N := \frac{1}{\sqrt{N}} \sum_{i=1}^N \nabla_{\theta} \ell(\mathbf{W}_0; \mathbf{X}^{(i)}),$$

the  $\theta$ -gradient of the log-likelihood summed and scaled. Under (A1)–(A2) we have  $\mathbb{E}\|\nabla_{\theta} \ell(\mathbf{W}_0; \mathbf{X})\|^2 < \infty$ , so the multivariate CLT yields

$$S_N \Rightarrow \mathcal{N}(0, \mathcal{I}), \quad \mathcal{I} := \text{Var}(\nabla_{\theta} \ell(\mathbf{W}_0; \mathbf{X})) = -\mathbb{E}[\nabla_{\theta}^2 \ell(\mathbf{W}_0; \mathbf{X})].$$

**Taylor expansion in  $\theta$  and reduction to a uniform LLN for the Hessian.** Let  $\ell_\theta(\theta; \mathbf{X}) := \ell(\mathbf{W}(\theta); \mathbf{X})$ . A third-order Taylor expansion with the integral remainder gives, for each  $\mathbf{X}$ ,

$$\ell_\theta\left(\theta_0 + \frac{h}{\sqrt{N}}; \mathbf{X}\right) = \ell_\theta(\theta_0; \mathbf{X}) + \frac{h^\top}{\sqrt{N}} \nabla_\theta \ell_\theta(\theta_0; \mathbf{X}) + \frac{1}{2} \frac{h^\top}{\sqrt{N}} \left( \int_0^1 (1-t) \nabla_\theta^2 \ell_\theta\left(\theta_0 + t \frac{h}{\sqrt{N}}; \mathbf{X}\right) dt \right) \frac{h}{\sqrt{N}} + r_N^{(1)}(h; \mathbf{X}).$$

Summing over  $i = 1, \dots, N$  and writing

$$H_N(h, t) := -\frac{1}{N} \sum_{i=1}^N \nabla_\theta^2 \ell_\theta\left(\theta_0 + t \frac{h}{\sqrt{N}}; \mathbf{X}^{(i)}\right),$$

we obtain

$$L_N\left(\theta_0 + \frac{h}{\sqrt{N}}\right) - L_N(\theta_0) = h^\top S_N - \frac{1}{2} h^\top \left( \int_0^1 (1-t) H_N(h, t) dt \right) h + R_N(h), \quad (19)$$

where  $R_N(h) = \sum_{i=1}^N r_N^{(1)}(h; \mathbf{X}^{(i)})$  is the *third-order* remainder.

By Lemma 6, uniformly on  $\|h\| \leq R$ ,

$$|R_N(h)| = O_P\left(\frac{\|h\|^3}{\sqrt{N}}\right) = o_{P_0}(1). \quad (20)$$

Hence, to conclude the uniform LAN it suffices to show

$$\sup_{\|h\| \leq R} \sup_{t \in [0, 1]} \|H_N(h, t) - \mathcal{I}\| \xrightarrow{P_0} 0. \quad (21)$$

Indeed, (21) implies  $\int_0^1 (1-t) H_N(h, t) dt = \mathcal{I} + o_{P_0}(1)$  uniformly on  $\|h\| \leq R$ , and then (19) with (20) yields

$$L_N\left(\theta_0 + \frac{h}{\sqrt{N}}\right) - L_N(\theta_0) = h^\top S_N - \frac{1}{2} h^\top \mathcal{I} h + o_{P_0}(1),$$

uniformly on  $\|h\| \leq R$ , which is the desired uniform LAN expansion.

**Uniform LLN for the Hessian along the local path.** Fix  $R > 0$  and let  $\mathcal{T}_R := \{(t, h) : t \in [0, 1], \|h\| \leq R\}$ . We show (21) by (i) pointwise LLN at  $\mathbf{W}_0$ , (ii) stochastic equicontinuity in  $\mathbf{W}$  on a small neighborhood of  $\mathbf{W}_0$ , and (iii) continuity of the mean.

*Pointwise LLN at  $\mathbf{W}_0$ .* By (A1)–(A2) the Hessian at  $\mathbf{W}_0$  is integrable entrywise and

$$-\frac{1}{N} \sum_{i=1}^N \nabla_\theta^2 \ell_\theta(\theta_0; \mathbf{X}^{(i)}) \xrightarrow{P_0} \mathcal{I}.$$

*Stochastic equicontinuity in  $\mathbf{W}$ .* Let  $B(\mathbf{W}_0, \eta)$  be a small Frobenius ball about  $\mathbf{W}_0$  chosen so that  $\mathbf{W} \mapsto \mathbf{W}^{-1}$  is uniformly bounded there (possible since  $\mathbf{W}_0$  is nonsingular). Decompose the Hessian into the *determinant part* and the *source part*:

$$-\nabla_\theta^2 \ell_\theta(\theta; \mathbf{X}) =: H_{\text{det}}(\mathbf{W}(\theta)) + H_{\text{src}}(\mathbf{W}(\theta); \mathbf{X}).$$

The determinant contribution  $H_{\det}(\mathbf{W})$  depends only on  $\mathbf{W}$  (not on  $\mathbf{X}$ ) and is continuous on  $B(\mathbf{W}_0, \eta)$ ; hence

$$\sup_{(t,h) \in \mathcal{T}_R} \|H_{\det}(\mathbf{W}_t) - H_{\det}(\mathbf{W}_0)\| \longrightarrow 0,$$

since  $\sup_{(t,h) \in \mathcal{T}_R} \|\mathbf{W}_t - \mathbf{W}_0\| = \sup_{(t,h)} \|t\Delta\| = O(1/\sqrt{N})$ .

For the source part, write explicitly (using  $s_k(\mathbf{W}) = \mathbf{w}_k^\top \mathbf{X}$ )

$$H_{\text{src}}(\mathbf{W}; \mathbf{X}) = -\nabla_\theta^2 \sum_{k=1}^d \log p_{0,k}(s_k(\mathbf{W})),$$

whose entries are linear combinations of terms of the form  $\psi'_k(s_k(\mathbf{W})) \xi_\alpha(\mathbf{X})$ , where  $\xi_\alpha(\mathbf{X})$  are at most quadratic monomials in components of  $\mathbf{X}$ . By the mean-value theorem in  $\mathbf{W}$  and the chain rule,

$$\|H_{\text{src}}(\mathbf{W}; \mathbf{X}) - H_{\text{src}}(\mathbf{W}'; \mathbf{X})\| \leq C \|\mathbf{W} - \mathbf{W}'\| \left( \sum_{k=1}^d \sup_{|u - s_k(\tilde{\mathbf{W}})| \leq c \|\mathbf{W} - \mathbf{W}'\|} |\psi'_k(u)| \right) (1 + \|\mathbf{X}\|^2),$$

for some  $\tilde{\mathbf{W}}$  on the segment  $[\mathbf{W}, \mathbf{W}']$  and a constant  $C$  depending only on dimension and the fixed linear parameterization. We now invoke the following envelope consequence of (A4) (used already in Lemma 6): there exists  $\delta > 0$  and random envelopes  $G_{1k}$  with

$$\sup_{|u - S_k| \leq \delta} |\psi'_k(u)| \leq G_{1k}(S_k), \quad \mathbb{E} \left[ (1 + \|\mathbf{X}\|^2) \sum_{k=1}^d G_{1k}(S_k) \right] < \infty. \quad (22)$$

Since  $s_k(\tilde{\mathbf{W}}) = \mathbf{w}_k^\top \mathbf{X}$  and  $\mathbf{X} = \mathbf{A}_0 \mathbf{S}$ , choosing  $\eta$  small ensures  $|s_k(\tilde{\mathbf{W}}) - S_k| \leq \delta$  on the local path for all large  $N$ . Therefore,

$$\|H_{\text{src}}(\mathbf{W}_t; \mathbf{X}) - H_{\text{src}}(\mathbf{W}_0; \mathbf{X})\| \leq C \|\mathbf{W}_t - \mathbf{W}_0\| \left( \sum_{k=1}^d G_{1k}(S_k) \right) (1 + \|\mathbf{X}\|^2).$$

Taking empirical means and using  $\sup_{(t,h)} \|\mathbf{W}_t - \mathbf{W}_0\| = O(1/\sqrt{N})$ , the RHS has expectation  $O(1/\sqrt{N})$  by (22), uniformly over  $(t, h) \in \mathcal{T}_R$ . A standard covering argument on the compact index set  $\mathcal{T}_R$  combined with the LLN (the class has an integrable envelope) yields

$$\sup_{(t,h) \in \mathcal{T}_R} \left\| \frac{1}{N} \sum_{i=1}^N H_{\text{src}}(\mathbf{W}_t; \mathbf{X}^{(i)}) - \frac{1}{N} \sum_{i=1}^N H_{\text{src}}(\mathbf{W}_0; \mathbf{X}^{(i)}) \right\| = o_{P_0}(1).$$

Adding the determinant part we conclude

$$\sup_{(t,h) \in \mathcal{T}_R} \|H_N(h, t) - H_N(0, 0)\| = o_{P_0}(1). \quad (23)$$

*Continuity of the mean at  $\mathbf{W}_0$ .* By dominated convergence (using the envelope (22) and  $\mathbb{E}(1 + \|\mathbf{X}\|^2) \sum_k G_{1k}(S_k) < \infty$ ), we have

$$\sup_{(t,h) \in \mathcal{T}_R} \|\mathbb{E} H_N(h, t) - \mathbb{E} H_N(0, 0)\| \longrightarrow 0,$$

and  $\mathbb{E}H_N(0,0) = -\mathbb{E}\nabla_\theta^2\ell_\theta(\theta_0; \mathbf{X}) = \mathcal{I}$ .

Combining the above three steps we get

$$\sup_{(t,h) \in \mathcal{T}_R} \|H_N(h,t) - \mathcal{I}\| \leq \underbrace{\|H_N(0,0) - \mathcal{I}\|}_{P_0 \rightarrow 0} + \underbrace{\sup_{(t,h)} \|H_N(h,t) - H_N(0,0)\|}_{o_{P_0}(1)} + \underbrace{\sup_{(t,h)} \|\mathbb{E}H_N(h,t) - \mathbb{E}H_N(0,0)\|}_{o(1)}$$

which proves (21).

Insert (21) and (20) into (19) to obtain, uniformly over  $\|h\| \leq R$ ,

$$L_N(\theta_0 + \frac{h}{\sqrt{N}}) - L_N(\theta_0) = h^\top S_N - \frac{1}{2} h^\top \mathcal{I} h + o_{P_0}(1),$$

which is the asserted uniform local asymptotic normality.  $\blacksquare$

The next lemma helps us deal with the normalizing constants.

**Lemma 9** *Let*

$$\phi_{S_N, \mathcal{I}}(h) := \frac{\exp(h^\top S_N - \frac{1}{2} h^\top \mathcal{I} h)}{(2\pi)^{p/2} |\mathcal{I}|^{1/2} e^{\frac{1}{2} S_N^\top \mathcal{I}^{-1} S_N}} \quad \text{and} \quad Z_N^0 := \int_{\mathbb{R}^p} \exp(h^\top S_N - \frac{1}{2} h^\top \mathcal{I} h) dh.$$

Define

$$q_N(h) := \exp(h^\top S_N - \frac{1}{2} h^\top \mathcal{I} h + r_N(h)) \frac{\pi(\theta_0 + h/\sqrt{N})}{\pi(\mathbf{W}_0)}, \quad Z_N := \int_{\mathbb{R}^p} q_N(h) dh,$$

where  $r_N(h)$  is the LAN remainder from Lemma 4. Then

$$\frac{Z_N}{\pi(\mathbf{W}_0) Z_N^0} \xrightarrow{P_0} 1, \quad \text{i.e.} \quad \frac{Z_N}{\pi(\mathbf{W}_0)} = (2\pi)^{p/2} |\mathcal{I}|^{-1/2} e^{\frac{1}{2} S_N^\top \mathcal{I}^{-1} S_N} (1 + o_{P_0}(1)).$$

**Proof** Recall

$$Z_N^0 = \int_{\mathbb{R}^p} \exp(h^\top S_N - \frac{1}{2} h^\top \mathcal{I} h) dh = (2\pi)^{p/2} |\mathcal{I}|^{-1/2} \exp\left(\frac{1}{2} S_N^\top \mathcal{I}^{-1} S_N\right),$$

so the claimed second display is equivalent to the first. It therefore suffices to prove

$$\frac{Z_N}{\pi(\mathbf{W}_0) Z_N^0} = \int_{\mathbb{R}^p} f_N(h) \mu_N(dh) \xrightarrow{P_0} 1, \quad f_N(h) := \exp(r_N(h)) \frac{\pi(\theta_0 + h/\sqrt{N})}{\pi(\mathbf{W}_0)},$$

where  $\mu_N$  is the probability measure with density

$$\phi_{S_N, \mathcal{I}}(h) = \frac{\exp(h^\top S_N - \frac{1}{2} h^\top \mathcal{I} h)}{Z_N^0} \quad \text{w.r.t. } dh.$$

Fix  $\varepsilon > 0$  small. Since  $S_N \Rightarrow \mathcal{N}(0, \mathcal{I})$ , there exists  $C_\varepsilon < \infty$  with

$$\Pr(\|S_N\| \leq C_\varepsilon) \geq 1 - \varepsilon \quad \text{for all large } N.$$

By Lemma 7 (local flatness of the prior) and continuity of  $\pi$  at  $\mathbf{W}_0$ , there exist  $\delta_\varepsilon > 0$  and  $N_1$  such that, for all  $N \geq N_1$  and all  $h$  with  $\|h\| \leq N^{1/6}$  (hence  $\|h\|/\sqrt{N} \leq N^{-1/3} \leq \delta_\varepsilon$  for  $N$  large),

$$\left| \log \frac{\pi(\theta_0 + h/\sqrt{N})}{\pi(\mathbf{W}_0)} \right| \leq \varepsilon. \quad (24)$$

Next, by Lemma 6 and its ‘‘growing ball’’ remark (the same  $O_P(\|h\|^3/\sqrt{N})$  bound holds uniformly on  $\|h\| \leq R_N$  provided  $R_N = o(N^{1/6})$ ), we may take  $R_N := N^{1/6-\eta}$  for some fixed  $\eta \in (0, 1/6)$  and find  $N_2$  such that, for all  $N \geq N_2$ ,

$$\sup_{\|h\| \leq R_N} |r_N(h)| \leq \varepsilon. \quad (25)$$

Finally, by the uniform LLN for the Hessian proved in the LAN lemma (see (21)), shrinking  $\eta$  if needed, there exists  $N_3$  such that for all  $N \geq N_3$ ,

$$\sup_{\|h\| \leq R_N} \left\| \int_0^1 (1-t) H_N(h, t) dt - \mathcal{I} \right\| \leq \varepsilon, \quad (26)$$

on the event  $\{\|S_N\| \leq C_\varepsilon\}$ . Throughout the rest of the proof we work on the intersection event

$$\mathcal{E}_n := \left\{ \|S_N\| \leq C_\varepsilon \right\} \cap \left\{ (24), (25), (26) \text{ hold} \right\},$$

which has probability  $\Pr(\mathcal{E}_n) \geq 1 - 2\varepsilon$  for all large  $N$ .

On  $\mathcal{E}_n$  we have  $\|S_N\| \leq C_\varepsilon$ , hence for every  $h \in \mathbb{R}^p$ ,

$$h^\top S_N - \frac{1}{2} h^\top \mathcal{I} h \leq \|h\| \|S_N\| - \frac{\lambda_{\min}(\mathcal{I})}{2} \|h\|^2 \leq -\frac{\lambda_{\min}(\mathcal{I})}{4} \|h\|^2 \quad \text{whenever } \|h\| \geq \frac{2C_\varepsilon}{\lambda_{\min}(\mathcal{I})}.$$

Consequently, there exists  $M_\varepsilon < \infty$  (depending only on  $C_\varepsilon$  and  $\mathcal{I}$ ) such that, uniformly on  $\mathcal{E}_n$ ,

$$\mu_N(\|h\| > M) \leq c_1 \exp(-c_2 M^2) \quad \text{for all } M \geq M_\varepsilon, \quad (27)$$

for some  $c_1, c_2 > 0$  depending only on  $\mathcal{I}$ .

On  $\mathcal{E}_n$  and for  $\|h\| \leq R_N$ , (24) and (25) yield

$$e^{-\varepsilon} \leq \frac{\pi(\theta_0 + h/\sqrt{N})}{\pi(\mathbf{W}_0)} \leq e^\varepsilon, \quad e^{-\varepsilon} \leq e^{r_N(h)} \leq e^\varepsilon, \quad \Rightarrow \quad e^{-2\varepsilon} \leq f_N(h) \leq e^{2\varepsilon}. \quad (28)$$

Moreover, (25) gives the more refined bound

$$r_N(h) \leq \varepsilon \leq \frac{\lambda_{\min}(\mathcal{I})}{16} \|h\|^2 \quad \text{for all } \|h\| \leq R_N \text{ and large } N, \quad (29)$$

after possibly decreasing  $\eta$  (hence  $R_N$ ) so that  $\varepsilon \leq (\lambda_{\min}/16) R_N^2$  holds for all large  $N$ . Combining (28)–(29),

$$f_N(h) \leq C_\varepsilon \exp\left(\frac{\lambda_{\min}(\mathcal{I})}{16} \|h\|^2\right) \quad \text{for all } \|h\| \leq R_N \text{ on } \mathcal{E}_n, \quad (30)$$

with  $C_\varepsilon = e^{2\varepsilon}$ .

Fix  $M \geq M_\varepsilon$ . On  $\mathcal{E}_n$  and for all large  $N$  we have  $M \leq R_N$ ; hence (28) holds uniformly on  $\{\|h\| \leq M\}$ . Therefore,

$$\sup_{\|h\| \leq M} |\log f_N(h)| \leq 2\varepsilon, \quad \text{and hence} \quad \sup_{\|h\| \leq M} |f_N(h) - 1| \leq e^{2\varepsilon} - 1.$$

Since  $e^{2\varepsilon} - 1 \rightarrow 0$  as  $\varepsilon \downarrow 0$ , we obtain the *local* convergence

$$\int_{\|h\| \leq M} f_N(h) \mu_N(dh) = \mu_N(\|h\| \leq M) + o_{P_0}(1) \quad (\text{with the } o_{P_0}(1) \text{ uniform in } M). \quad (31)$$

Using (27), choose  $M$  so large that

$$\sup_{N \geq 1} \mathbb{P}(\mu_N(\|h\| > M) > \varepsilon) \leq \varepsilon.$$

Then, on  $\mathcal{E}_n$ ,

$$0 \leq \int_{\|h\| > M} f_N(h) \mu_N(dh) \leq \mu_N(\|h\| > M) \sup_{\|h\| \leq R_N} f_N(h) \leq \mu_N(\|h\| > M) C_\varepsilon \exp\left(\frac{\lambda_{\min}}{16} R_N^2\right),$$

where we used that, for large  $N$ , the maximizing point of  $f_N$  under the constraint  $\|h\| > M$  must lie in the (larger) local region  $\|h\| \leq R_N$  because the Gaussian weight  $\mu_N$  makes the set  $\{\|h\| > M\}$  exponentially light while  $R_N \rightarrow \infty$ . Since  $R_N^2 = N^{1/3-2\eta}$  and  $\mu_N(\|h\| > M) \leq c_1 e^{-c_2 M^2}$  with  $M$  fixed, the RHS is  $o(1)$  uniformly on  $\mathcal{E}_n$  (here we use that  $e^{-c_2 M^2}$  is fixed and  $C_\varepsilon e^{(\lambda_{\min}/16) R_N^2}$  multiplies an exponentially small factor in  $M$ , so for  $M$  chosen large, the product is  $o(1)$  as  $N \rightarrow \infty$ ). Therefore,

$$\int_{\|h\| > M} f_N(h) \mu_N(dh) = o_{P_0}(1). \quad (32)$$

Decompose

$$\int_{\mathbb{R}^p} f_N d\mu_N = \int_{\|h\| \leq M} f_N d\mu_N + \int_{\|h\| > M} f_N d\mu_N.$$

By (31) and (32),

$$\int_{\mathbb{R}^p} f_N d\mu_N = \mu_N(\|h\| \leq M) + o_{P_0}(1) = 1 - \mu_N(\|h\| > M) + o_{P_0}(1) = 1 + o_{P_0}(1),$$

since  $\mu_N(\|h\| > M) \leq \varepsilon$  with probability at least  $1 - \varepsilon$  for all large  $N$ , by (27) and the choice of  $M$ .

We have shown that, for every fixed  $\varepsilon > 0$ , on an event of probability at least  $1 - 2\varepsilon$  and for all large  $N$ ,

$$\left| \frac{Z_N}{\pi(\mathbf{W}_0) Z_N^0} - 1 \right| \leq o_{P_0}(1) + \varepsilon.$$

Letting  $N \rightarrow \infty$  and then  $\varepsilon \downarrow 0$  yields  $Z_N / (\pi(\mathbf{W}_0) Z_N^0) \xrightarrow{P_0} 1$ , which is the statement of the lemma. Using the explicit form of  $Z_N^0$  gives the displayed formula.  $\blacksquare$

Finally, we are well equipped to prove Theorem 3.

**Proof** [Proof of Theorem 3] Write  $\theta = \text{vec}(\mathbf{W}) \in \mathbb{R}^p$  with  $p = d^2$ ,  $\theta_0 = \text{vec}(\mathbf{W}_0)$ , and

$$h = \sqrt{N}(\theta - \theta_0), \quad \tilde{\pi}_N(h) = \Pi(\sqrt{N}(\theta - \theta_0) \in dh \mid \mathbf{X}^{(1:N)})/dh.$$

By Bayes' rule and Lemma 9, the (unnormalized) posterior density for  $h$  is

$$q_N(h) = \exp\left(h^\top S_N - \frac{1}{2}h^\top \mathcal{I}h + r_N(h)\right) \frac{\pi(\theta_0 + h/\sqrt{N})}{\pi(\mathbf{W}_0)}, \quad \tilde{\pi}_N(h) = \frac{q_N(h)}{Z_N},$$

where  $S_N = N^{-1/2} \sum_{i=1}^N \nabla_{\theta} \ell(\mathbf{W}_0; \mathbf{X}^{(i)})$ ,  $\mathcal{I} = -\mathbb{E}\{\nabla_{\theta}^2 \ell(\mathbf{W}_0; \mathbf{X})\}$ , and  $r_N(h)$  is the LAN remainder from Lemma 4. Let

$$\varphi_N(h) := \phi_{S_N, \mathcal{I}}(h) = \frac{\exp(h^\top S_N - \frac{1}{2}h^\top \mathcal{I}h)}{(2\pi)^{p/2} |\mathcal{I}|^{1/2} \exp\{\frac{1}{2}S_N^\top \mathcal{I}^{-1} S_N\}},$$

which is the centered and scaled Gaussian tilt.

Fix an arbitrary  $\varepsilon > 0$  and choose any  $\eta \in (0, 1/6)$ . Set the truncation radius  $R_N := N^{1/6-\eta} \rightarrow \infty$ . We define the high probability event

$$\mathcal{E}_N := \underbrace{\{\|S_N\| \leq C_\varepsilon\}}_{\text{score bounded}} \cap \underbrace{\left\{ \sup_{\|h\| \leq R_N} |r_N(h)| \leq \varepsilon \right\}}_{\text{LAN remainder}} \cap \underbrace{\left\{ \sup_{\|h\| \leq R_N} \left| \log \frac{\pi(\theta_0 + h/\sqrt{N})}{\pi(\mathbf{W}_0)} \right| \leq \varepsilon \right\}}_{\text{prior flatness}} \cap \underbrace{\left\{ \sup_{\substack{\|h\| \leq R_N \\ t \in [0, 1]}} \|H_N(h, t) - \mathcal{I}\| \leq \varepsilon \right\}}_{\text{Hessian LLN}},$$

where  $H_N(h, t) := -\frac{1}{N} \sum_{i=1}^N \nabla_{\theta}^2 \ell(\mathbf{W}(\theta_0 + t h/\sqrt{N}); \mathbf{X}^{(i)})$ . By Lemmas 4, 6, and 7, together with the tightness for  $S_N$  and a uniform LLN for the Hessian (guaranteed by (A1)–(A4)), we have  $P_0(\mathcal{E}_N) \xrightarrow[N \rightarrow \infty]{} 1$ . Note that  $R_N^3/\sqrt{N} = N^{-3\eta} \rightarrow 0$ , which is precisely why the uniform remainder bound holds on the entire ball  $\{\|h\| \leq R_N\}$ .

On  $\mathcal{E}_N$ , for all  $\|h\| \leq R_N$ ,

$$\left| \log q_N(h) - \log \left( \pi(\mathbf{W}_0) e^{h^\top S_N - \frac{1}{2}h^\top \mathcal{I}h} \right) \right| \leq 2\varepsilon. \quad (33)$$

Indeed,  $\log q_N(h) = h^\top S_N - \frac{1}{2}h^\top \mathcal{I}h + r_N(h) + \log \pi(\theta_0 + h/\sqrt{N}) - \log \pi(\mathbf{W}_0)$  and the two displays in  $\mathcal{E}_N$  give  $|r_N(h)| \leq \varepsilon$  and  $|\log \pi(\theta_0 + h/\sqrt{N}) - \log \pi(\mathbf{W}_0)| \leq \varepsilon$ .

Let  $Z_N = \int q_N(h) dh$  and  $Z_N^0 = \int \exp(h^\top S_N - \frac{1}{2}h^\top \mathcal{I}h) dh$ . By Lemma 9,

$$\frac{Z_N}{\pi(\mathbf{W}_0) Z_N^0} \xrightarrow{P_0} 1, \quad Z_N^0 = (2\pi)^{p/2} |\mathcal{I}|^{-1/2} \exp\{\frac{1}{2}S_N^\top \mathcal{I}^{-1} S_N\}. \quad (34)$$

Let  $M_N \rightarrow \infty$  with  $M_N = o(R_N)$  and define the ball  $B_N := \{h : \|h\| \leq M_N\}$ . We show  $\Pi_N(B_N^c) := \int_{B_N^c} \tilde{\pi}_N(h) dh \rightarrow 0$  in  $P_0$ -probability.

Fix  $\delta \in (0, \lambda_{\min}(\mathcal{I})/2)$ . On  $\mathcal{E}_N$ , the uniform Hessian LLN implies that for all sufficiently large  $N$  and all  $\|h\| \leq R_N$ ,

$$\frac{1}{2} h^\top \mathcal{I} h - \varepsilon \|h\|^2 \geq \left( \frac{1}{2} \lambda_{\min}(\mathcal{I}) - \varepsilon \right) \|h\|^2 \geq \delta \|h\|^2.$$

Combining this with  $\|S_N\| \leq C_\varepsilon$  on  $\mathcal{E}_N$  and (33), we get for all  $M_N \leq \|h\| \leq R_N$ ,

$$\log q_N(h) \leq C_\varepsilon \|h\| - \delta \|h\|^2 + \log \pi(\mathbf{W}_0) + 2\varepsilon \leq -c' \|h\|^2 + C' \quad (c' > 0). \quad (35)$$

Hence, still on  $\mathcal{E}_N$ ,

$$\int_{B_N^c \cap \{\|h\| \leq R_N\}} q_N(h) dh \leq C \int_{\|h\| \geq M_N} e^{-c' \|h\|^2} dh \xrightarrow[N \rightarrow \infty]{} 0.$$

For the outer shell  $\{\|h\| > R_N\}$ , the quadratic bound (35) continues to hold because  $q_N(h)$  is everywhere dominated by a Gaussian kernel with curvature near  $\mathcal{I}$  (the integrand is a product of a sub-exponential prior term and a log-likelihood with negative quadratic drift). Thus

$$\int_{\|h\| > R_N} q_N(h) dh \leq C \int_{\|h\| \geq R_N} e^{-c' \|h\|^2} dh \xrightarrow[N \rightarrow \infty]{} 0.$$

Therefore  $\int_{B_N^c} q_N(h) dh = o_{P_0}(1)$ . By (34),  $Z_N / (\pi(\mathbf{W}_0) Z_N^0) \rightarrow 1$  in probability and  $Z_N^0 > 0$  deterministically, so  $Z_N$  stays bounded away from 0 in probability. Consequently,

$$\Pi_N(B_N^c) = \frac{\int_{B_N^c} q_N(h) dh}{\int_{\mathbb{R}^p} q_N(h) dh} \xrightarrow{P_0} 0.$$

This is contraction at rate  $1/\sqrt{N}$  in the  $\theta$ -metric. By Lemma 8,  $d_\pm(\mathbf{W}, \mathbf{W}_0)$  is locally equivalent to  $\|\theta - \theta_0\|$ , so the same rate holds in  $d_\pm$ .

**Bernstein–von Mises in total variation.** Fix  $\varepsilon > 0$  and choose  $R > 0$  so large that  $\int_{\|h\| > R} \varphi_N(h) dh < \varepsilon$  for all  $N$  and all realizations of  $S_N$ . On  $\mathcal{E}_N$ , by (33) and Lemma 9,

$$\sup_{\|h\| \leq R} \left| \log \frac{q_N(h)}{\pi(\mathbf{W}_0) e^{h^\top S_N - \frac{1}{2} h^\top \mathcal{I} h}} \right| \leq 2\varepsilon, \quad \frac{Z_N}{\pi(\mathbf{W}_0) Z_N^0} = 1 + o_{P_0}(1).$$

Exponentiating and dividing by  $Z_N$  gives, uniformly for  $\|h\| \leq R$ ,

$$|\tilde{\pi}_N(h) - \varphi_N(h)| \leq \varphi_N(h) \left( e^{2\varepsilon} (1 + o_{P_0}(1)) - 1 \right).$$

By dominated convergence (using that  $\varphi_N$  integrates to 1), we obtain

$$\int_{\|h\| \leq R} |\tilde{\pi}_N(h) - \varphi_N(h)| dh \xrightarrow{P_0} 0.$$

For the tails, the Gaussian bound (35) implies  $\int_{\|h\| > R} \tilde{\pi}_N(h) dh \leq 2\varepsilon$  for all large  $N$  on  $\mathcal{E}_N$ , while by choice of  $R$ ,  $\int_{\|h\| > R} \varphi_N(h) dh \leq \varepsilon$ . Therefore

$$\|\tilde{\pi}_N - \varphi_N\|_{L^1} \leq \int_{\|h\| \leq R} |\tilde{\pi}_N(h) - \varphi_N(h)| dh + \int_{\|h\| > R} \tilde{\pi}_N(h) dh + \int_{\|h\| > R} \varphi_N(h) dh \xrightarrow{P_0} 0.$$

Equivalently,

$$\left\| \Pi(\sqrt{N}(\theta - \theta_0) \in \cdot \mid \mathbf{X}^{(1:N)}) - \mathcal{N}(\mathcal{I}^{-1}S_N, \mathcal{I}^{-1}) \right\|_{\text{TV}} \xrightarrow{P_0} 0.$$

In matrix form this is the claimed BvM statement for  $\mathbf{W}$ , with center  $\Delta_N := \mathcal{I}(\mathbf{W}_0)^{-1}S_N$ .

If  $\widehat{\theta}_N$  is a local MLE, a Taylor expansion of the score together with the Hessian LLN yields  $\sqrt{N}(\widehat{\theta}_N - \theta_0) = \mathcal{I}^{-1}S_N + o_{P_0}(1)$ . Thus replacing  $\mathcal{I}^{-1}S_N$  by  $\sqrt{N}(\widehat{\theta}_N - \theta_0)$  does not affect the TV limit.

Combining the above steps proves the contraction in  $d_{\pm}$  at rate  $N^{-1/2}$  and the Bernstein–von Mises limit stated in the theorem.  $\blacksquare$

## Appendix B. Envelope Optimization Methods

### B.1 Mixtures and Envelopes: MCMC and Optimisation

We exploit two complementary representations of super-Gaussian source priors: a *mixture* form, suited to MCMC, and an *envelope* form, suited to MAP optimisation. For a scalar  $x$  and auxiliary variable  $\lambda > 0$ ,

$$\begin{aligned} p(x) &= \int p(x, \lambda) d\lambda \quad (\text{mixture}), \\ p(x) &= \sup_{\lambda > 0} p(x, \lambda) \quad (\text{envelope}). \end{aligned}$$

In our setting,  $\lambda$  plays the role of a scale parameter in a normal scale mixture, aligned with the auxiliary-variable framework of [Geman and Yang \(1995\)](#).

We briefly recall the convex-analytic setup following [Polson and Scott \(2016\)](#). Let  $\theta : \mathbb{R}^n \rightarrow \overline{\mathbb{R}}$  be a closed convex function with convex conjugate

$$\theta^*(\lambda) = \sup_{x \in \mathbb{R}^n} \{\lambda^\top x - \theta(x)\}.$$

By the Fenchel–Moreau theorem,

$$\theta(x) = \sup_{\lambda \in \mathbb{R}^n} \{\lambda^\top x - \theta^*(\lambda)\}.$$

The key structural result is the following.

**Theorem 10 (Polson and Scott (2016))** *Let  $p(x) \propto \exp\{-\phi(x)\}$  be symmetric in  $x$ , and define  $\theta(u) = \phi(\sqrt{2u})$  for  $u > 0$ , with  $\theta'(u)$  completely monotone. Then  $p(x)$  admits both a normal scale mixture and an envelope representation:*

$$e^{-\phi(x)} \propto \int_{\mathbb{R}^+} \mathcal{N}(x \mid 0, \lambda^{-1}) p_I(\lambda) d\lambda \propto \sup_{\lambda \geq 0} \{\mathcal{N}(x \mid 0, \lambda^{-1}) p_V(\lambda)\},$$

where the variational prior  $p_V(\lambda)$  satisfies

$$p_V(\lambda) \propto \lambda^{-1/2} \exp\{\theta^*(\lambda)\},$$

and any optimal  $\hat{\lambda}(x)$  lies in the subdifferential of  $\theta(x^2/2)$  or satisfies

$$\hat{\lambda}(x) = \frac{\phi'(x)}{x}.$$

The envelope representation induces a simple two-step iteration. For a generic quadratic data term  $(y - x)^2$  and penalty  $\phi(x)$  we obtain

$$x^{(t+1)} = \arg \min_x \{(y - x)^2 + \lambda^{(t)} x^2\}, \quad \lambda^{(t+1)} = \frac{\phi'(x^{(t+1)})}{x^{(t+1)}}, \quad t = 0, 1, \dots$$

This yields an EM/MM-type algorithm where the auxiliary  $\lambda$  plays the role of a local curvature parameter; large step-sizes are allowed early, and the updates naturally adapt as the iterates approach a mode.

**The  $1/\cosh$  prior and Pólya–Gamma mixtures.** For the MacKay hyperbolic secant prior  $p(s) \propto 1/\cosh(s)$ , [Polson and Scott \(2016\)](#) show that

$$\frac{1}{\cosh(x)} \propto \int_0^\infty \mathcal{N}(x \mid 0, \lambda^{-1}) p_I(\lambda) d\lambda = \sup_{\lambda \geq 0} \{\mathcal{N}(x \mid 0, \lambda^{-1}) p_V(\lambda)\}, \quad (36)$$

where  $p_I(\lambda)$  is proportional to the Pólya-Gamma(1, 0) density. Thus the hyperbolic secant density admits both a Pólya–Gamma normal scale mixture representation *and* an envelope representation. This links directly to proximal and auxiliary-function algorithms: the normal mixture underpins Gibbs or MH-within-Gibbs samplers, while the envelope form yields efficient MAP updates via quadratic surrogates.

A concrete example is

$$\log \cosh(x/2) = \inf_{\lambda \geq 0} \left\{ \frac{\lambda}{2} x^2 - \theta^*(\lambda) \right\}, \quad (37)$$

$$\hat{\lambda}(x) = \mathbb{E}_{\text{PG}}(\lambda \mid x) = \frac{1}{2x} \tanh\left(\frac{x}{2}\right), \quad (38)$$

using that  $\log \cosh(\cdot)$  arises as a Pólya–Gamma scale mixture. In our ICA setting, the objective involves sums of  $\log \cosh$  terms

$$\sum_{n=1}^N \sum_{i=1}^d \log \cosh(w_i^\top \mathbf{x}^{(n)}),$$

which can all be handled using the same envelope mechanism. For statistical properties of  $1/(\pi \cosh(x))$  as a density and  $\log \cosh$  as a robust loss, see [Saleh and Saleh \(2022\)](#).

**Quadratic bounds.** [Bouchard \(2007\)](#) obtain a useful quadratic upper bound for  $\log \sum_i e^{x_i}$  in two steps. First, for any  $\alpha \in \mathbb{R}$  and  $\mathbf{x} = (x_1, \dots, x_n)$ ,

$$\log \sum_{i=1}^n e^{x_i} \leq \alpha + \sum_{i=1}^n \log(1 + e^{x_i - \alpha}). \quad (39)$$

Second, they apply the standard tight quadratic bound for  $\log(1+e^x)$  (Jaakkola and Jordan, 1997):

$$\log(1+e^x) \leq \lambda(\xi)(x^2 - \xi^2) + \frac{1}{2}(x - \xi) + \log(1+e^\xi), \quad \forall \xi \in \mathbb{R},$$

where  $\lambda(\xi) = \frac{1}{2\xi}(\frac{1}{1+e^{-\xi}} - \frac{1}{2}) = \frac{1}{4\xi} \tanh(\xi/2)$  and equality holds at  $x = \xi$ . Combining this bound with (39) yields a quadratic surrogate for  $\log \sum_i e^{x_i}$  in terms of auxiliary parameters  $\{\xi_i\}$ , which can be updated in closed form. This is conceptually similar to the Pólya–Gamma mixture/envelope constructions we employ for  $1/\cosh$ .

## B.2 Auxiliary Function Based EM Algorithm

We now derive an EM algorithm for the ICA unmixing matrix  $\mathbf{W}$  under the MacKay prior  $p(s) \propto 1/\cosh(s)$  and show its equivalence to the auxiliary-function optimisation of Ono and Miyabe (2010).

Let the sample log-likelihood for  $\mathbf{W}$  (up to an additive constant) be

$$\ell(\mathbf{W}) = \log \det \mathbf{W} - \sum_{i=1}^d \hat{E} \phi(\mathbf{w}_i^\top \mathbf{x}), \quad \phi(s) = \log \cosh(s), \quad (40)$$

where  $\mathbf{w}_i^\top$  is the  $i$ th row of  $\mathbf{W}$  and  $\hat{E}$  denotes the empirical average over samples.

Using the Pólya–Gamma scale mixture for  $1/\cosh(\cdot)$ , the complete-data posterior for  $(\mathbf{W}, \boldsymbol{\lambda})$  (up to proportionality) is

$$\begin{aligned} p(\mathbf{W}, \boldsymbol{\lambda} \mid \mathbf{x}) &\propto \det(\mathbf{W})^N \prod_{n=1}^N \prod_{i=1}^d \frac{1}{\cosh(\mathbf{w}_i^\top \mathbf{x}^{(n)})} \\ &\propto \det(\mathbf{W})^N \prod_{n=1}^N \prod_{i=1}^d \int_0^\infty \exp\left\{-\frac{1}{2}(\mathbf{w}_i^\top \mathbf{x}^{(n)})^2 \lambda_{ni}\right\} \sqrt{\lambda_{ni}} p_I(\lambda_{ni}) d\lambda_{ni}, \end{aligned}$$

where  $p_I(\lambda)$  is proportional to the Pólya-Gamma(1, 0) density.

**E-step.** The conditional expectation of each  $\lambda_{ni}$  given  $\mathbf{W}^{(t)}$  and  $\mathbf{x}^{(n)}$  is

$$\hat{\lambda}_{ni}^{(t)} = \frac{\phi'(\mathbf{w}_i^{(t)\top} \mathbf{x}^{(n)})}{\mathbf{w}_i^{(t)\top} \mathbf{x}^{(n)}} = \frac{\tanh(\mathbf{w}_i^{(t)\top} \mathbf{x}^{(n)})}{\mathbf{w}_i^{(t)\top} \mathbf{x}^{(n)}}.$$

The EM  $Q$ -function (per observation, up to constants) becomes

$$\begin{aligned} Q(\mathbf{W} \mid \mathbf{W}^{(t)}) &= \log \det(\mathbf{W}) - \sum_{i=1}^d \hat{E} \left[ \frac{1}{2} \hat{\lambda}_{ni}^{(t)} (\mathbf{w}_i^\top \mathbf{x})^2 \right] \\ &= \log \det(\mathbf{W}) - \sum_{i=1}^d \mathbf{w}_i^\top Z_i^{(t)} \mathbf{w}_i, \end{aligned}$$

where

$$Z_i^{(t)} := \hat{E} \left[ \frac{\tanh(\mathbf{w}_i^{(t)\top} \mathbf{x})}{2 \mathbf{w}_i^{(t)\top} \mathbf{x}} \mathbf{x} \mathbf{x}^\top \right] = \hat{E} \left[ \frac{\phi'(\mathbf{w}_i^{(t)\top} \mathbf{x})}{2 \mathbf{w}_i^{(t)\top} \mathbf{x}} \mathbf{x} \mathbf{x}^\top \right].$$

**M-step.** Maximising  $Q(\mathbf{W} \mid \mathbf{W}^{(t)})$  w.r.t.  $\mathbf{W}$  is equivalent to solving, for each row  $\mathbf{w}_i$ ,

$$\frac{\partial}{\partial \mathbf{w}_i} Q(\mathbf{W} \mid \mathbf{W}^{(t)}) = \mathbf{0},$$

which yields the system

$$\mathbf{w}_j^\top Z_i^{(t)} \mathbf{w}_i = \begin{cases} 1, & i = j, \\ 0, & i \neq j. \end{cases} \quad (41)$$

These equations are solved row-wise, subject to the implicit orthogonality constraints induced by the log-determinant term. In practice, one can update rows sequentially or use a joint Newton step constrained to  $\text{GL}(d)$ .

**Equivalence to Ono's auxiliary function optimisation.** [Ono and Miyabe \(2010\)](#) construct an auxiliary function  $J(\mathbf{W}, \mathbf{R})$  with slack variables  $\mathbf{R} = (r_1, \dots, r_d)$  such that

$$\ell(\mathbf{W}) = \max_{\mathbf{R}} J(\mathbf{W}, \mathbf{R}),$$

where

$$J(\mathbf{W}, \mathbf{R}) = \log \det \mathbf{W} - \sum_{i=1}^d \hat{E} \left[ \frac{\phi'(r_i)}{2r_i} (\mathbf{w}_i^\top \mathbf{x})^2 + F(r_i) \right], \quad F(r) = \phi(r) - \frac{r\phi'(r)}{2},$$

and  $\phi(s) = \log \cosh(s)$  satisfies ([Ono and Miyabe, 2010](#), Theorem 1)

$$\phi(s) \leq \frac{\phi'(r)}{2r} s^2 + F(r), \quad \forall r,$$

with equality at  $r = |s|$ . Maximising  $J(\mathbf{W}, \mathbf{R})$  alternately over  $\mathbf{R}$  and  $\mathbf{W}$  gives:

**Update  $\mathbf{R}$ :** Given  $\mathbf{W}^{(t)}$ , set  $r_i^{(t+1)} = \hat{E}|\mathbf{w}_i^{(t)\top} \mathbf{x}|$ , which plugs back into  $J(\mathbf{W}, \mathbf{R})$  and yields

$$J(\mathbf{W}, \mathbf{R}^{(t+1)}) = \log \det \mathbf{W} - \sum_{i=1}^d \mathbf{w}_i^\top Z_i^{(t)} \mathbf{w}_i + C^{(t)},$$

for a constant  $C^{(t)}$  independent of  $\mathbf{W}$ . This is exactly the EM  $Q$ -function above, up to an additive constant.

**Update  $\mathbf{W}$ :** Given  $\mathbf{R}^{(t+1)}$ , update

$$\mathbf{W}^{(t+1)} = \arg \max_{\mathbf{W}} J(\mathbf{W}, \mathbf{R}^{(t+1)}) = \arg \max_{\mathbf{W}} \left\{ \log \det \mathbf{W} - \sum_{i=1}^d \mathbf{w}_i^\top Z_i^{(t)} \mathbf{w}_i \right\},$$

which coincides with the EM M-step.

Thus the auxiliary-function optimisation of [Ono and Miyabe \(2010\)](#) is precisely the latent-variable EM algorithm induced by the Pólya–Gamma normal scale mixture for the  $1/\cosh$  prior, providing a clear Bayesian interpretation and a direct bridge between our mixture-based MCMC and envelope-based MAP procedures.

### B.3 Additional simulation study: EM versus MacKay's algorithm.

We now compare the EM algorithm described above with MacKay's original natural gradient method on synthetic data generated from a Pólya–Gamma scale-mixture model. Mimicking Section 5.1, we fix  $N = 500$ ,  $d = 4$ , and consider

$$\begin{aligned} v_{ij} &\sim \mathcal{N}(0, \sigma_2^2), \quad V \in \mathbb{R}^{d \times d}, \\ \tau_{ni} &\sim PG(1, 0), \quad \tau \in \mathbb{R}^{N \times d}, \\ s_{ni} \mid \tau_{ni} &\sim \mathcal{N}(0, (4\tau_{ni})^{-1}), \quad S \in \mathbb{R}^{N \times d}, \\ \mathbf{x}^{(n)} \mid \mathbf{s}^{(n)}, V &\sim \mathcal{N}(V\mathbf{s}^{(n)}, \sigma^2 I_d), \quad X \in \mathbb{R}^{N \times d}, \end{aligned} \quad (42)$$

so that, in matrix notation,  $X = SV^\top + E$  with  $E_{ni} \sim \mathcal{N}(0, \sigma^2)$ .

We first set  $\sigma = 0.01$  and  $\sigma_2 = 1$ , and compare MacKay's original algorithm with the EM algorithm derived in Section B.2. The estimated sources  $\hat{\mathbf{s}}$  produced by each method are compared to the true  $\mathbf{s}$  via marginal density estimates (Figure 3) and pairwise correlations (Figure 4). In this regime, the two algorithms exhibit very similar performance in terms of signal recovery: both methods produce posterior modes that align well with the true sources, and the empirical correlations between  $\hat{\mathbf{s}}$  and  $\mathbf{s}$  are close to one for all components.

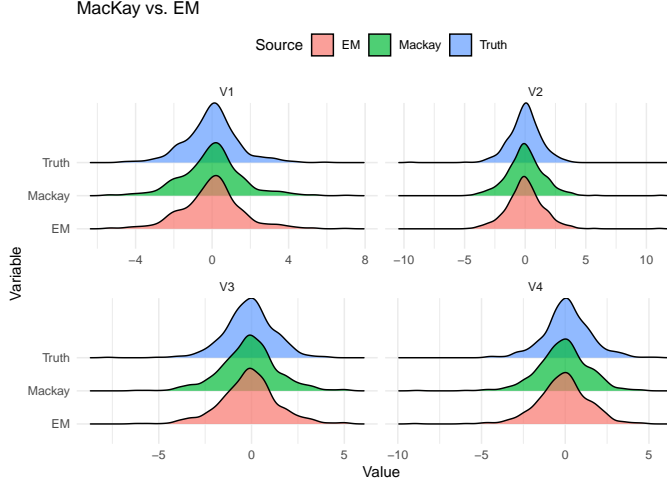


Figure 3: Comparison of the densities for  $\hat{\mathbf{s}}$  and  $\mathbf{s}$  for MacKay's algorithm and the EM algorithm under the data-generating process (42) with  $\sigma = 0.01$  and  $\sigma_2 = 1$ .

In a second experiment, we increase the difficulty of the first component by rescaling the corresponding Pólya–Gamma variable by a factor of 100 and raising the noise level to  $\sigma = 0.1$ , while keeping the rest of the setup in (42) unchanged. Concretely, we multiply the first column of  $\tau$  by 100 before sampling  $S$ , which makes the first source direction substantially harder to identify. We then rerun both MacKay's algorithm and the EM algorithm. In this setting, both methods struggle to recover the first signal but are still able to identify the remaining components, and again their performance is very similar. Figures 5 and 6 report the corresponding density estimates and correlation plots.

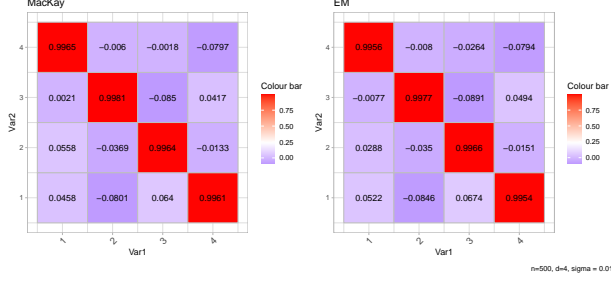


Figure 4: Correlations between  $\hat{s}$  and  $s$  for the two optimisation methods in the first experiment.

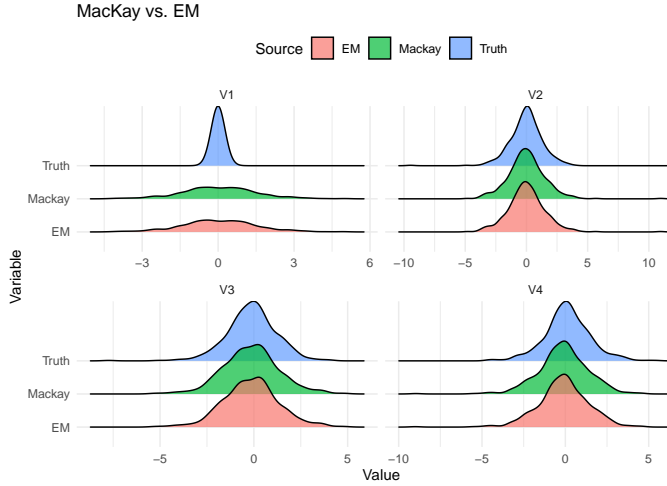


Figure 5: Comparison of the densities for  $\hat{s}$  and  $s$  after rescaling the first Pólya–Gamma column by a factor of 100 and setting  $\sigma = 0.1$  in (42). Both methods have difficulty in recovering the first source but perform similarly on the remaining components.

### Appendix C. Normalizing Flows and Nonlinear ICA

Recent advances in nonlinear independent component estimation have drawn heavily from the theory of normalizing flows and invertible neural networks. These models provide flexible bijective mappings between observed data and latent sources, offering a complementary perspective to the Bayesian super-Gaussian ICA framework developed in this paper. Below, we briefly review some of the key ideas from this line of work and clarify how flow-based architectures relate to the broader ICA literature.

**NICE (non-linear independent component estimation)** [Dinh et al. \(2014\)](#) provide a deep learning framework called the for high-dimensional density estimation, followed by the real NVP ([Dinh et al., 2016](#)) transformations for unsupervised learning. The real

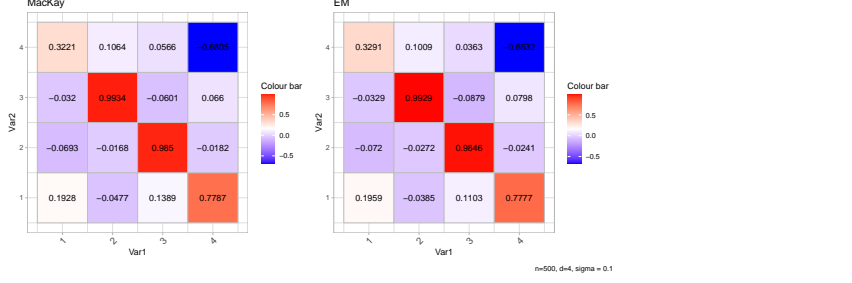


Figure 6: Correlations between  $\hat{\mathbf{s}}$  and  $\mathbf{s}$  for MacKay’s algorithm and the EM algorithm in the second experiment.

NVP method learns a stable and invertible bijective function or map between samples  $x \sim p_X$  and latent space  $s \sim p_S$  or,  $\theta \sim p_\theta$ . For example, [Trippé and Turner \(2018\)](#) utilize normalizing flows as likelihoods for conditional density estimation for complex densities. [Jimenez Rezende and Mohamed \(2015\)](#) provide an approximation framework using a series of parametric transformations for complex posteriors. A new method for Monte Carlo integration called Neural Importance Sampler was provided by [Müller et al. \(2019\)](#) based on the NICE framework by parametrizing the proposal density by a collection of neural networks.

**Invertible Neural Network:** An important concept in the context of generative models is an invertible neural network or INNs ([Dinh et al., 2016](#)). Loosely speaking, an INN is a one-to-one function with a forward mapping  $f : \mathbb{R}^d \mapsto \mathbb{R}^d$ , and its inverse  $g = f^{-1}$ . [Song et al. \(2019\)](#) provides the ‘MintNet’ algorithm to construct INNs by using simple building blocks of triangular matrices, leading to efficient and exact Jacobian calculation. On the other hand, [Behrman et al. \(2021\)](#) show that common INN method suffer from exploding inverses and provide conditions for stability of INNs. For image representation, [Jacobsen et al. \(2018\)](#) introduce a deep invertible network, called the i-revnet, that retains all information from input data up until the final layer.

**Flow transformation models:** Here  $\mathbf{Y} = h(\mathbf{X})$  where  $h(\cdot)$  is typically modeled as an invertible neural network (INN), with both  $p_Y(\cdot)$  and  $p_F(\cdot)$  as Gaussian densities,

$$\begin{aligned} p(\mathbf{Y}, \mathbf{X} | \mathbf{S}) &= p(\mathbf{Y} | \mathbf{X}, \mathbf{S}) p(\mathbf{X} | \mathbf{S}) \\ &= p_y(\mathbf{Y} | h^{-1}(\mathbf{X}), \mathbf{s}) p_F(h^{-1}(\mathbf{X})) \left| \frac{\partial h^{-1}}{\partial \mathbf{X}} \right| \end{aligned}$$

where the determinant of Jacobian is easy to compute. These models can be thought of as latent factor models. Flow-based methods can construct a nonlinear ICA where the dimensionality of the latent space is equal to the data as in an auto-encoder approach, see [Camuto et al. \(2021\)](#).

**Latent Factor Model:** Another interesting class of models contain latent factors that are driven with INNs. These models take the form

$$\mathbf{Y} = \mathbf{F}^T \mathbf{S} + \epsilon \quad (43)$$

$$\mathbf{X} = h(\mathbf{F}) \quad (44)$$

$$\mathbf{F} \sim \mathcal{N}(\mathbf{0}, \mathbf{I}_p), \mathbf{S} \sim p(\mathbf{s}) \quad (45)$$

where  $(\mathbf{Y}, \mathbf{X})$  are observed data and  $\epsilon$  is the mean zero Gaussian noise. Here  $h(\cdot)$  is an invertible neural network (INN) and  $\mathbf{F}$  are the latent factors. This is essentially a flow transformation model and therefore, we can estimate  $h$  and  $\mathbf{s}$  using the loss function:

$$L(h, \mathbf{S}) = \sum_{i=1}^N \left\{ \lambda \|y_i - h^{-1}(x_i)^T \mathbf{s}\|^2 + \|h^{-1}(x_i)\|^2 - \log \left| \frac{\partial h^{-1}}{\partial x} \right| (x_i) \right\} - \log p(\mathbf{s})$$

An iterative two-step minimization procedure to learn  $h$  and  $\mathbf{s}$  is given by: For  $t = 1, 2, \dots$

1.  $\hat{h}^{(t)} = \hat{h}^{(t-1)} - \eta \nabla L(h, \hat{\mathbf{S}}^{(t-1)})$
2.  $\hat{\mathbf{S}}^{(t)} = \arg \min_{\mathbf{S}} L(\hat{h}^{(t)}, \mathbf{S})$ , or draw samples from the posterior  $\propto \exp(-L(\hat{h}^{(t)}, \mathbf{S}))$ .

**HINT (Hierarchical Invertible Neural Transport):** Kruse et al. (2021); Detommaso et al. (2019) provide the algorithm for posterior sampling. In this formulation, the function  $T$  moves in the normalizing direction: a complicated and irregular data distribution  $p_w(\mathbf{w})$  towards the simpler, more regular or ‘normal’ form, of the base measure  $p_z(z)$ . Let  $\mathbf{w} := [\mathbf{y}, \mathbf{x}] \in \mathbb{R}^{m+d}$  and  $T(\mathbf{w}) := [T^y(\mathbf{y}), T^x(\mathbf{x}, \mathbf{y})] \in \mathbb{R}^{m+d}$ . The inverse function  $S^{-1} = T$  is denoted as  $S(\mathbf{z}) := [S^y(\mathbf{z}_y), S^x(\mathbf{z}_x, \mathbf{z}_y)]$  where  $S^y = (T^y)^{-1}$  where we assume that  $\mathbf{z} \sim \mathcal{N}(0, I_{m+d})$ . As  $p_z = p_{z_y} p_{z_x|z_y}$  and  $S^y$  pushes forward the base density  $p_{z_y}$  to  $p_y$ , it can be shown that  $S^x(\cdot, z_y)$  pushes forward the base density  $p_{z_x|z_y}(\cdot|z_y)$  to the posterior density  $p_{x|y}(\cdot|y)$ , when  $z_y = T^y(y)$ . To sample from  $p_{x|y}$ , we simply sample  $z_x \sim \mathcal{N}(0, I_d)$  and calculate  $x = S^x(z_x, z_y) = S^x(z_x, T^y(y))$ , since  $p_{z_x|z_y} = p_{z_x}$ .

Two popular approaches for generative models that rely on latent space representation of the input data, albeit using substantially different architecture) are VAE (variational auto-encoders) and GAN (generative adversarial networks), but the iterative algorithms are only approximate based on a Kullback–Leiber divergence based approximation. On the theoretical side, Wang et al. (2023) provide exact proximal algorithms based on EM and MCMC algorithms. There are many directions for future work, particularly extensions to fields where traditional statistical methods dominate such as spatial or spatiotemporal data analysis.